4. AUTOMOTIVE METALS—TITANIUM

A. Low-Cost Titanium Powder for Feedstock

Principal Investigators: Curt A. Lavender and K. Scott Weil
Pacific Northwest National Laboratory
P.O. Box 999, Richland, WA 99352
(509) 372-6770; fax: (509) 375-4448; e-mail: curt.lavender@pnl.gov
(509) 375-6796; fax: (509) 375-4448; e-mail: scott.weil@pnl.gov

Technology Area Development Manager: Joseph A. Carpenter
(202) 586-1022; fax: (202) 586-1600; e-mail: joseph.carpenter@ee.doe.gov

Field Technical Monitor: Mark T. Smith
(509) 375-4478; fax: (509) 375-4448; e-mail: mark.smith@pnl.gov

---

Contractor: Pacific Northwest National Laboratory
Contract No.: DE-AC06-76RLO1830

Objectives

- Investigate alternate powder and melt processing methods for low-cost titanium (Ti) materials.
- Evaluate processing methods to produce powder metallurgy Ti products with International Titanium Powder, Inc. (ITP) powder.
- Evaluate the suitability of emerging Ti technologies for the production of low-cost Ti products for automotive applications.

Approach

- Perform characterization and analysis of the sintering behavior of the ITP powder. Provide feedback of results to ITP for use in process design.
- Develop low-cost feedstocks for powder metallurgy (P/M) use in automotive applications from low-cost Ti tetrachloride ($TiCl_4$).
- Survey the emerging technologies for the low-cost production of Ti powders and evaluate for use in automotive applications.

Accomplishments

- A Ti powder containing only vanadium as a beta stabilizer produced using the ITP process was obtained, characterized by scanning electron microscope and X-Ray diffraction and evaluated for sinterability.
- Developed press-and-sinter cycles that produced greater than 97% dense plates of cold-pressed Ti from the ITP powder.
- Developed sintering cycles that produced 95+% dense bars of commercial purity (CP) Ti that exhibit ductility of up to 14% in selected samples from standard tensile tests using low-cost $TiCl_4$.
- A low-cost precursor for the alloying addition of iron to the ITP process has been identified.
- A series of die and powder lubricants based on aromatic hydrocarbons was evaluated and increased green density of the Hunter fines powder, resulting in an increase from 90 to 94+% of theoretical as-sintered density.

Future Direction

- Perform cost analysis on two new emerging Ti production processes and update the ITP process cost model.
- Perform laboratory trials of sodium reduction of an iron precursor as a low-cost beta stabilizer for the ITP process.
- Produce a beta stabilized alloy bar for use in automotive applications using a powder produced by a low-cost process.
- Measure tensile and fatigue properties of low-cost beta alloy bar stock.
- Continue the development of sintering cycles for the ITP powder with an emphasis on understanding the sintering mechanisms of the powder to increase ductility.
- The Ti4V alloy powder is to be evaluated and processed powder will be characterized for tensile properties.

Introduction

This project is a collaborative effort between Ford, General Motors, Chrysler, Pacific Northwest National Laboratory (PNNL) and the Ti raw material producers and is focused on the development and evaluation of low-cost feedstock materials produced by emerging low-cost Ti production technologies. The purpose of this project is to develop and demonstrate materials and processing methods for producing low-cost Ti feedstock materials and automotive components. The project will evaluate and validate all processing steps necessary to produce low-cost Ti materials capable of meeting automotive property requirements.

Metal products fabricated from Ti possess a combination of properties that could substantially increase the performance and reduce the mass of automobiles. Although Ti has been used in low production volume specialty and racing automobiles, widespread use of Ti in higher volume production vehicles has been prevented by the high expense of producing Ti components. The cost to extract Ti metal from beach sand by the conventional Kroll process alone exceed the cost targets needed for most automotive uses. Several new processes for the production of Ti metal have been developed in recent years and are projected to meet the cost targets of the automotive industry. This project will survey the Ti industry for emerging technologies and evaluate their suitability as feedstock for automotive applications through technical cost studies and characterization.

Many of the newly developed processes produce Ti in a powder product ready for use in the solid-state consolidation processes. Solid-state Ti consolidation by P/M methods will substantially reduce the secondary processing costs by the elimination of energy intensive and low yielding conventional ingot processing technology. Because each new process produces a powder with unique processing requirements and because there is virtually no commercial Ti P/M industry, PNNL will perform processing trials on each powder product that has been projected to satisfy the automotive cost goals.

Approach

The earlier phase of this project was focused on the selection of low-cost powder and secondary processing development. The current phase will be directed at the production of semi-finished products of automotive interest.

Results and Discussion

Due to its relatively high strength, Ti alloys are the most likely materials to be substituted for high-strength steels in applications such as fasteners and suspension components [1]. To date, this project has focused on the development of low-cost feed materials for use in the emerging power production technologies. Although low-cost interstitial elements such as carbon, oxygen and nitrogen are used to strengthen commercial purity Ti, corresponding decreases in ductility, fracture toughness and fatigue strength require the use of an alloy. Using conventional ingot metallurgy processing, commercial purity Ti sponge is

blended with master alloy chunks, which are then pressed into a compact that is vacuum arc or electron beam melted. The ingots are then forged to refine the as-cast microstructure and processed to a semi-finished shape such as a bar or rod. The production of this semi-finished product from ingot usually results in a yield loss on the order of 50%. This process is costly, requiring the development of expensive raw material feedstocks and high purity master alloys. The primary advantage of the newly developed processes is that they produce Ti in a powder form that can be used in solid-state consolidation at a near-net shape and in the case of P/M, net-shape products.

During this reporting period, the project focused on the challenges associated with development of high-yield low-cost beta Ti alloy processing, and evaluation of die and pressing friction associated with direct P/M processing.

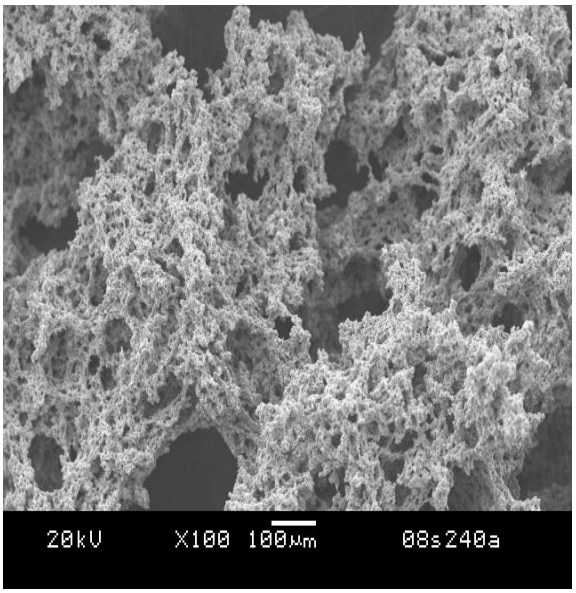

Figure 1. Low-cost Ti4V powder morphology as produced by ITP.

Beta Titanium Alloys

Beta Ti alloys are made by alloying with an element that allows the retention of body centered cubic beta phase at room temperature after rapid cooling from above the beta transus [2]. Beta alloys are normally "age" hardened to high strength (i.e., above 1400 megaPascals (MPa) by the low temperature transformation of beta to the alpha phase [3]. Typically, alloying elements such as molybdenum that stabilize beta are costly, but an effective beta stabilizer is iron, which would be a low-cost addition, possibly lowering the overall alloy cost. As a beta stabilizer, iron presents several challenges; therefore, for ease of processing at ITP the initial trial of beta alloy production was a binary alloy containing only 4 weight percent vanadium (Ti4V). The vanadium was added using a halide that co-reduced efficiently with $TiCl_4$ and produced the pre-alloyed powder shown in Figure 1.

The Ti4V as shown in Figure 2(a) appeared similar in morphology to the commercial purity powders (CP Ti) produced previously and shown in Figure 2(b). The powders were characterized by energy dispersive x-ray (EDX) in the scanning electron microscope (SEM) to evaluate the distribution of the vanadium. As determined by EDAX analysis, the vanadium appears to be

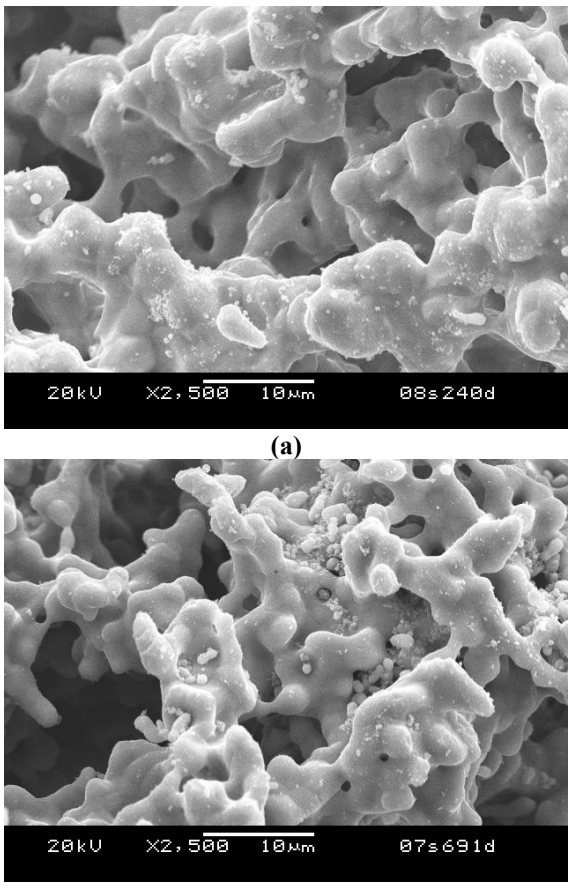

Figure 2. (a) SEM micrographs of low-cost commercial purity and (b) low-cost Ti4V powder showing similar morphology.

uniformly distributed, and it would be expected that the alloy is relatively homogeneous given the amount of vanadium solid solution. The powder was then X-rayed to determine which phase (alpha or beta) had been produced during cooling from the reduction process. The x-ray peaks shown in Figure 3 indicate that both alpha and beta were stabilized [4].

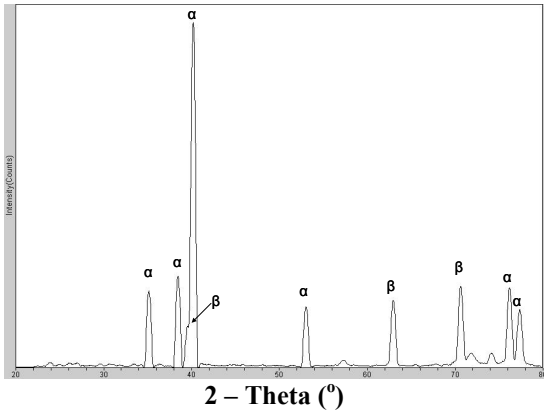

Figure 3. X-Ray of as-produced Ti4V powder, showing the presence of both alpha and beta phase.

The sinterability of the Ti4V was found to be superior to commercial purity powder. In like sinter conditions, the Ti4V consistently sintered to greater than 97% dense, compared to 91% for the CP Ti. This result is likely related to the same mechanism observed in low purity $TiCl_4$, where the vanadium raises the onset of sintering and allows deleterious species to off-gas prior to closing porosity as shown in the dilatometry presented in Figure 4. Although the shrinkage curves shown by Figure 4 show only slight difference, the distinction is in a critical region where many Na compounds tend to decompose, allowing gases to escape prior to a closed porosity condition. Heat treatment studies and tensile testing will be performed, and the sintered Ti4V tensile bars will be measured.

Beta Alloy Bar Stock

Ti is projected to replace high-strength steel fasteners and suspensions components in automotive applications; therefore, a low-cost method to produce bar stock must be developed.

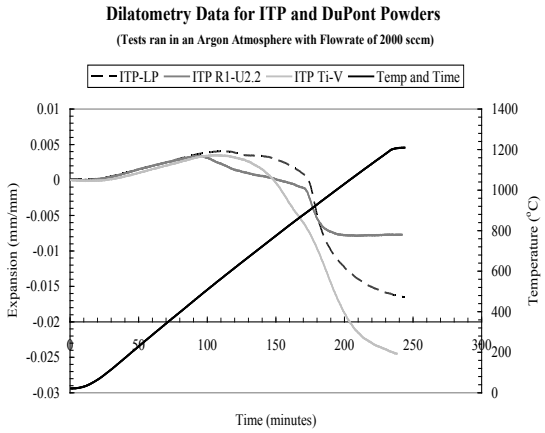

Figure 4. Sintering shrinkage curves powders produced from low-cost $TiCl_4$ (ITP-LP), refined $TiCl_4$ (ITP-R1-U2.2) and Ti with 4 weight percent vanadium.

Conveniently, the new Ti production processes produce powders that can be consolidated by solid state processing. Several studies have looked at solid state consolidation by extrusion; however, the studies are primarily driven by aerospace applications that use irregular cross-section. For the automotive industry, the primary shape of interest will be a round bar stock made by a low-cost rod-rolling method. Therefore, a study has been initiated to produce alloys Ti64 (Ti6Al4V), Ti5553 (Ti5Al5V5Mo5Cr) and Ti185 (Ti1Al8V5Fe) by hot rod-rolling.

The Ti64 alloy was selected as a moderate strength baseline material. Although Ti5553 is not a low-cost composition, there are many extrusion studies that can be used for comparison for this high-strength alloy. Developed in the 1950s by Mallory-Sharon Titanium Company, the Ti185 alloy is a unique composition that when heat treated properly could develop strengths in excess that of Ti5553 with a low-cost composition that can be produced by the ITP process. The Ti185 development was stopped due to iron segregation that occurred during solidification, which may be prevented by using a low-cost P/M solid-state consolidation method resulting in a homogeneous high-strength alloy. The rods produced by this study will be characterized for fatigue, tensile strength and double shear compared to ingot-processed materials.

Low-cost Iron Precursor

Iron can be an effective beta stabilizer; however, iron can segregate during melting, leaving an inhomogeneous microstructure. The addition of iron to Ti by P/M can avoid the segregation and lead to homogeneous low-cost beta alloys. Although iron can be reduced during the ITP process, it is a more difficult element to add to the ITP process. An iron precursor that may be incorporated easily into the ITP process has been identified and is under evaluation. Conceptually in the ITP process, the iron precursor would be vaporized along with $TiCl_4$ to form a mixed-vapor steam. When injected into a spray of molten sodium, the $TiCl_4$ will react with the sodium to form Ti and NaCl, and the heat of reaction will cause the iron precursor to decompose thermally into zero valent iron, thus simultaneously generating the metal species needed to form a Ti-Fe alloy powder. PNNL researchers plan to carry out small-scale proof-of-principle experiments to validate the concept and to understand the variables involved in the overall reaction prior to attempting the process on a larger scale at ITP.

Powder Processing

Powder/Die Lubrication

Ti powders create many challenges for high-volume die pressing due to a high tendency to gall. Using a previously developed instrumented die and newly developed aromatic hydrocarbon lubricants, the coefficient of friction for the low-cost Ti powder has been reduced to below copper powders that are used in high volume production. In addition to decreased friction to levels that can be used in high-volume P/M die pressing, the green density of the compacts increased to levels greater than 90%, resulting in higher as-sintered densities and increased ductility. The progress in the die pressing is summarized in Figures 5 and 6, which show that Ti powders with admixed lubricant and die wall lubrication can be pressed with a coefficient of friction less than that of a copper alloy without issue in high-volume P/M processing and sintered to greater than 93% of theoretical density. As shown in Figure 5, the use of a powder lubricant can reduce the die wall friction to levels near those of high-production volume iron and copper powders and will allow

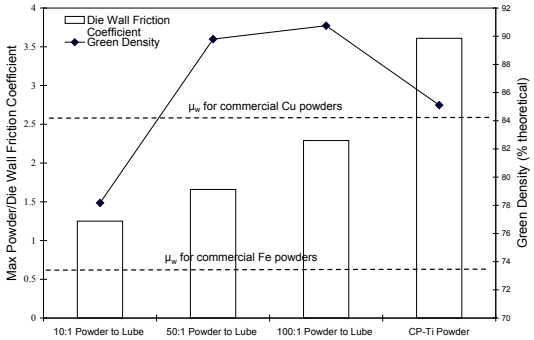

Figure 5. Summary pressing results using a double acting instrumented pressing die with anthracene. With proper lubrication, the low-cost Ti powders can behave similar to copper and iron powders used in high-volume P/M processing.

the use of Ti powders in automotive volume die pressing. Continued development of the powder lubrication is summarized in Figure 6, which shows that the preferred lubricant of Ti is camphor, an aromatic hydrocarbon whose complete removal occurred during sintering leaves behind no residual contamination.

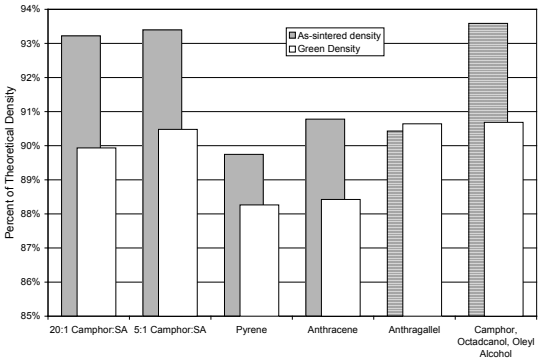

Figure 6. Density effects of various lubrication schemes mixed at a 50:1 with Ti powder.

Conclusions

The conclusions reached during this reporting period are as follows:

- As shown by the investigation of the Ti4V alloy, small alloying additions to the ITP powder process result in substantial differences in the sintering behavior of Ti powder. Combined with the previous results using the low-cost $TiCl_4$, this significant

conclusion suggests that an alloy could be tailored to produce low-cost Ti P/M components.
- Solid-state consolidation for beta bar stock will allow the use of low-cost alloys and processes previously not possible with ingot metallurgy processing.
- Powder lubrication with aromatic hydrocarbons will allow the use of Ti powder in high-volume die pressing applications. Friction can be reduced by a factor of 3 while raising the as-sintered density from 90 to 94%.

Presentations/Publications/Patents

1. S. Hong, Y. Hovanski, C. A. Lavender, and K. S. Weil. 2008. "Investigation of Die Stress Profiles during Powder Compaction using Instrumented Die." *J Materials Engineering and Performance* 17(3):382–386. DOI:10.1007/s11665-008-9229-1.
2. C. A. Lavender. 2008. "Titanium Recycle." USCAR Recycling Working Group Meeting, Detroit, MI. September 24.
3. M. Sadayappan, M. Sahoo, C. A. Lavender, and P. Jablonski. 2008. "Permanent Mold Casting of Titanium Alloy TI-6AL-4V." *Intl J of Metalcasting* 2(1):69–74.
4. K. S. Weil, Y. Hovanski, and C. A. Lavender. "Effects of TiCl4 purity on the sinterability of Armstrong-processed Ti powder." *J Alloys Compd*, DOI:10.1016/j.jallcom.2008.06.09.

References

1. Personal communication from Dr. Andrew Sherman, Ford Motor Company.
2. P. J. Bania. 1994. *J Met* 41:16–19.
3. Weiss and S. L. Semiatin. 1998. *Mat Sci A* A243:46–65.
4. J. W. Elmert et al. 2003. *J Appl Phys* 93(4):15. February.

B. Production of Heavy Vehicle Components from Low-Cost Titanium Powder

Principal Investigator: Seong Jin Park
Associate Research Professor
Center for Advanced Vehicular Systems, CAVS, 2215
Mississippi State University, P.O. Box 5405
Mississippi State, MS 39762-5405
(662) 325-8565; e-mail: sjpark@cavs.msstate.edu

Co-Principal Investigator: Haitham El Kadiri
Assistant Research Professor
Center for Advanced Vehicular Systems
Mississippi State University, P.O. Box 5405
Mississippi State, MS 39762-5405
(662) 325-5568; Cell: (662) 617-4790; e-mail: elkadiri@cavs.msstate.edu

Co-Principal Investigator: Youssef Hammi
Center for Advanced Vehicular Systems
Mississippi State University, P.O. Box 5405
Mississippi State, MS 39762-5405
(662) 325-5452; e-mail: yhammi@cavs.msstate.edu

Contractor: Mississippi State University (MSST)
Contract No.: 4000054701

Objective

- Design and produce titanium (Ti) structural components by using math-based, experimentally validated, powder compaction and sinter models.

Approach

- Examine lower cost blended elemental (BE) and prealloyed Ti powders that are responsive to the powder metallurgy process and synthesize new combinations and innovations in powders composition. Recent developments, such as using hydride powders, have enabled the fabrication of BE parts to over 99% of full density, resulting in significantly improved properties. Additives such as carbon or boron then can generate carbide or boride reinforcing phases—dispersed phase composites. Further studies and developments show that this approach may be well suited to reduce the cost of producing automotive parts, making titanium more cost competitive with other materials commonly used.
- Explore powder modifications, novel organometallic lubricants (the composition is proprietary), finite element analysis of compaction to minimize wall friction and wear, and evaluation of novel tooling materials and coatings. New computer tools for modeling porosity and size change during both compaction and sintering will be tailored to titanium systems with the ability of performing computer aided design for the tooling and processes to attain dense and net-shaped final products.

Accomplishments

- Completed a literature survey for low-cost Ti powder and Ti alloys for automotive application, including cost analyses and processing techniques.
- Designed new Ti alloys and proposed three Ti alloy candidates.

- Evaluated and selected Ti alloys including boride Ti alloys based on mechanical properties, liquid phase sinterability, and cost-effectiveness.
- Performed powder injection molding (PIM) experiment.
- Developed simulation tool for PIM, die compaction, sintering, and hot isostatic pressing (HIPing) with some optimization.

Future Direction

- Continue PIM experiment.
- Develop modeling and simulation for die compaction, sintering, and HIPing using Oak Ridge National Laboratory (ORNL) experimental data.
- Produce a real component for automotive use.

Introduction

Lower cost Ti could be the catalyst for titanium to break into the automotive industry. The goal is to have a competitively priced Ti component produced by cost-competitive manufacturing methods. The research on Ti and Ti-matrix composites is the first stage in a sequence of powder metallurgy (P/M) efforts geared to infuse net-shape production of lightweight materials into the domestic automotive industry. P/M techniques afford designers the ability to produce significantly complex near-net shape parts at potentially significant cost savings, with very little wasted material.

Table 1 shows the overall structure of Task 1 with ORNL collaboration.

Table 1. Overall structure of Task 1.

	Experiment	Simulation
Die compaction	ORNL	MSST
PIM	MSST	MSST
Sintering	ORNL	MSST
HIPing	ORNL	MSST

Work Schedule

Table 2 shows the current progress based on the schedule planned. Subtasks related to the experiment are at risk now because we need experimental data for die compaction, sintering, and HIPing for modeling. For the PIM, we need to find a sponge powder supplier or support from ORNL.

Table 2. The proposed schedule of Task 1 with marks of progress.

Subtasks	Year 1				Year 2			
	Q1	Q2	Q3	Q4	Q1	Q2	Q3	Q4
1.1 literature review, first simulation	100							
1.2 powder evaluation	100							
1.3 microstructure and interfacial study	100							
1.4 processing evaluation	100							
1.5 modeling and simulation		100						
1.6 optimization		75						
1.7 experimental verification		50						
1.8 mechanical properties					50			
1.9 process verification								

Summary of Progress

Task 1 consists of four research categories: literature survey, Ti alloy design and evaluation, PIM experiment, and modeling and simulation for Ti powder processing.

Literature Survey

The literature was surveyed for Ti powder production methods for gas atomized, hydride-dehydride (HDH), and sponge Ti powders; Ti alloys; P/M processes; and previous uses of Ti alloys for automotive applications. The cost of Ti alloys is at least 10 times higher than the cost of aluminum (Al) alloys and 30 times higher than the cost of steels. Table 3 summarizes the consumption of Ti alloys in the automotive market between 1998 and 2002. It can be seen that Ti alloys were never used in massive production mode but were limited only to components

Table 3. Ti alloy use in automotive applications.

Year	Component	Material	Manufacturer
1998	Brake guide pins	Grade 2	Mercedes
1998	Sealing washers	Grade 1s	Volkswagen
1998	Gear shift knob	Grade 1	Honda
1999	Connecting rods	Ti-6Al-4V	Porsche
1999	Valves	Ti-6Al-4V	Toyota
1999	Turbocharger rotor	Ti-6Al-4V	Mercedes
2000	Suspension spring	LCB	Volkswagen
2000	Valve cups	ß-Ti alloy	Mitsubishi
2000	Turbocharger rotor	γ-TiAl	Mitsubishi
2001	Exhaust system	Grade 2	GM
2002	Valves	Ti-6Al-4V	Nissan

requiring extra high stiffness and superior maximum strength and fatigue strength scaled to density. However, manufacturers show a preference for the more expensive Ti alloys over Al in powertrains if rotating and oscillating masses are to be substantially reduced.

We also analyzed the cost for the candidate Ti alloys, as shown in Figure 1. This analysis indicates that the Ti powder type is the most important factor in cost among gas atomized, HDH, and sponge Ti powders.

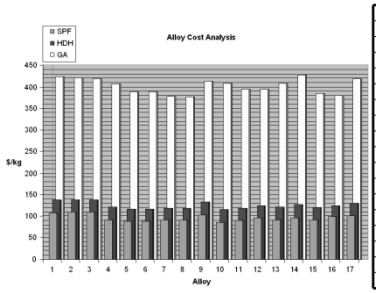

ID	Alloy Composition
1	Ti-6Al-4V
2	Ti-6Al-4V-1Mo
3	Ti-6Al-4V-1Mo-0.2B
4	Ti-8Al-1V-1Mo
5	Ti-6Al-2Sn-4Zr-2Mo
6	Ti-6Al-2Sn-4Zr-2Mo-0.2Si
7	Ti-6.5Al-4.6Sn-4.6Zr-1Nb-0.3Si-1Mo
8	Ti-6.6Al-4.6Sn-4.6Zr-0.9Nb-1Mo-0.35Si
9	Ti-4.5Al-3V-2Fe-2Mo
10	Ti-6Al-1.7Fe-0.1Si
11	Ti-4.5Fe-6.8Mo-1.5Al
12	Ti-1.5Fe-6.8Mo-4.8Al-1.2Nb
13	Ti-1Fe-1Mo-6.3Al-1.2Nb
14	Ti-1.5Fe-2.25Mo-1.2Nb-0.3Al
15	Ti-6Al-4Sn-4Zr-1Nb-1Mo-0.2Si
16	Ti-4.3Fe-7Mo-1.4Al-1.4V-5.4B
17	Ti-2Co-2Mo-1.4Al-1.4V-1.8B

Figure 1. Cost analysis plot for candidate Ti alloys.

Ti Alloy Design

Ti alloys can be a predominant monophase structure; hexagonal close-packed (hcp) or body-centered cubic (bcc), or a dual phase structure $\alpha + \beta$, depending on the composition strength ratio between the hcp stabilizing elements and bcc stabilizing elements. Figure 2 schematically illustrates the main properties of potential Ti alloys falling in different crystallographic classes. Alpha alloys only enclose traces of beta phase. Near-alpha alloys contain predominantly alpha,

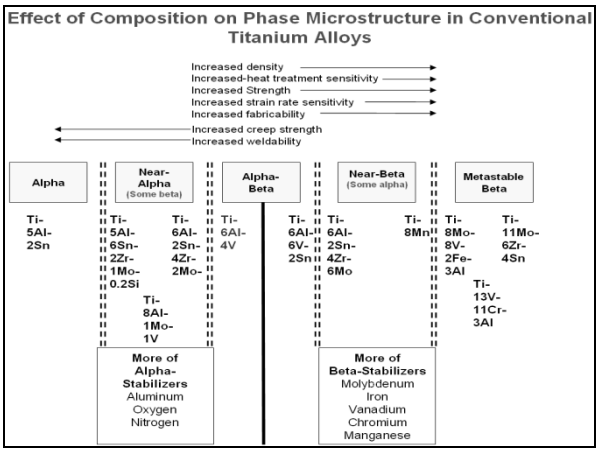

Figure 2. General classification of titanium alloys with respect to properties and microstructure.

and the microstructure may appear similar to that of an alpha alloy. A dual phase alpha-beta alloy consists of alpha and retained or partially transformed beta phases. Metastable beta alloys consist of predominantly retained beta, which is susceptible to a fine transformation upon post-heat treatments. All of these alloys are used for applications where temperatures are less than 600°C, although the melting temperature is higher than that of typical steel. The thermal expansion coefficient is less than half that of Al.

Based on our research, we recommend starting with the following three alloy compositions for generating the eutectic systems.

1. Ti- (2 to 3%)Fe- (3% to 6%)Zr- (2% to 4%)Sn- (1% to 3%)Mo- (0% to 1%Cr)
2. Ti- (2 to 3%)Fe- (3% to 6%)Zr- (2% to 4%)Sn- (2% to 3%)Mn- (1 to 2%)Mo- (0% to 1%Cr)
3. Ti- (2 to 3%)Fe- (3% to 6%)Zr- (2% to 4%)Sn- (2% to 3%)Mn- (1 to 2%)Mo- (2% to 5%)Cr3C2

Currently we have purchased these powders for evaluating the proposed Ti alloy compositions. The evaluation will be performed through powder mixing, die compaction, sintering, and mechanical property measurement. Figure 3 shows the optimization algorithm for liquid phase sintering of Ti alloy powder.

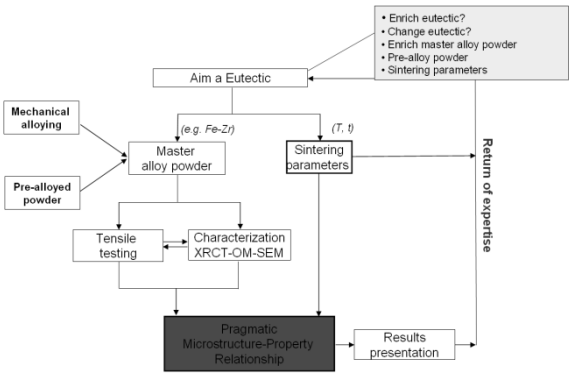

Figure 3. Composition optimization algorithm for liquid phase sintering of Ti alloy powder.

As for the PIM, we prepared PIM feedstock based on the standard wax-polymer binder system with 50% solid loading percentage. Now we are measuring the viscosity using a homemade capillary rheometer to obtain the material properties for the simulations.

Experimental Evaluation of Designed Ti Alloys

In this research, three different Ti powers are used as shown in Figure 4: (1) sponge (DuPont), (2) HDH (Phelly Materials), and (3) gas-atomized powders (Sumitomo Corporation). To evaluate the designed Ti alloys described in the previous section, we also purchased additive elements such as iron (Fe), molybdenum (Mo), zirconium (Zr), tin (Sn), manganese (Mn), chromium (Cr), and chromium carbide (Cr_2C_3).

We evaluated 15 Ti alloys as shown in Table 4 and selected 6 Ti alloys according to the following criteria (in order).

1. Higher sintered density using liquid phase sintering (LPS) cycle.
2. Clear endothermic peak for LPS (see Figure 5).
3. Cost of Ti alloys.

Based on the 6 selected Ti alloys, we proposed 16 Ti alloys with more/different combinations of additive elements. We measured the mechanical properties of the 16 Ti alloys, including sintered density, hardness, ultimate tensile strength, and

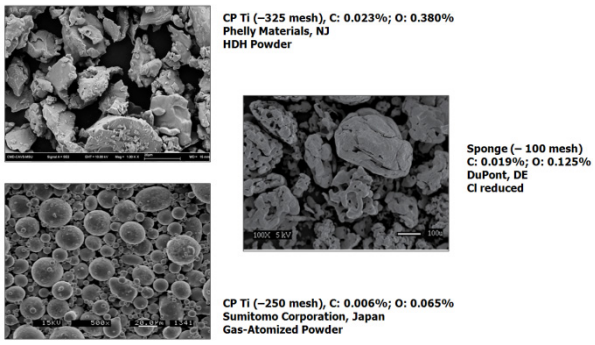

Figure 4. SEM images for three Ti powders used in this research.

Table 4. Ti alloys evaluated and selected.

ID No.		Ti	Fe %	Mo %	Zr %	Sn %	Mn %	Cr %	Cr_2C_3 %
1		97.0	1.5	1.5					
2		94.0	3.0	3.0					
3	selected	94.5	1.5	1.5	2.5				
4		89.0	3.0	3.0	5.0				
5	selected	93.0	1.5	1.5	2.5	1.5			
6		86.0	3.0	3.0	5.0	3.0			
7		91.5	1.5	1.5	2.5	1.5	1.5		
8	selected	83.0	3.0	3.0	5.0	3.0	3.0		
9		90.5	1.5	1.5	2.5	1.5	1.5	1.0	
10	selected	81.0	3.0	3.0	5.0	3.0	3.0	2.0	
11	selected	89.5	1.5	1.5	2.5	1.5	1.5	1.0	1.0
12		79.0	3.0	3.0	5.0	3.0	3.0	2.0	2.0
13	selected	83.0	3.0	3.0	6.0	4.0		1.0	
14		81.0	3.0	2.0	6.0	4.0	3.0	1.0	
15		76.0	3.0	3.0	6.0	4.0	3.0		5.0

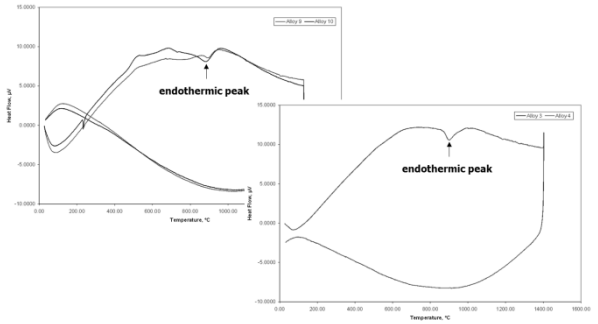

Figure 5. Differential scanning calorimetry experiment for LPS evaluation.

elongation, as shown in Table 5. Finally, we selected Ti-Fe-Zr combinations as candidate Ti alloys.

We focused on microstructural analysis of Ti-Fe-Zr alloys produced by the press and sinter process. Samples were produced by mixing of initial pure metallic powders followed by uniaxial pressing with subsequent densification by sintering at 1,275°C in vacuum. Scanning electron microscopy (SEM) and optical microscopy were used to study

Table 5. Mechanical properties for selected Ti alloys.

Alloy	Density (g/cm³)	Green Sample		Sintered Sample (1275 °C, 60 min, 10 mtorr)				
		Density (g/cm³)	Relative Density (%)	Density (g/cm³)	Relative Density (%)	Hardness (HRB)	elongation (%)	UTS (MPa)
Pure Ti	4.51	3.24	71.8	4.14	91.8	88.1	3.13	643
Ti-5Fe-2.5Zr	4.64	3.26	70.2	4.41	94.9	103.9	3.54	1025
Ti-5Fe-5Zr	4.68	3.29	70.3	4.40	94.0	104.3	2.50	1227
Ti-10Fe-2.5Zr	4.75	3.21	67.6	4.54	95.6	108.1	0.60	611
Ti-10Fe-5Zr	4.79	3.43	71.6	4.77	99.6	112.9	0.00	281
Ti-5Fe	4.61	3.39	73.6	4.30	93.3	101.7		
Ti-10Fe	4.71	3.26	69.2	4.40	93.4	104.5		
Ti-10Fe-2.5Zr-1Cr	4.77	3.21	67.3	4.37	91.7	102.6		
Ti-10Fe-5Zr-1Cr	4.81	3.34	69.5	4.43	92.2	104.4		
Ti-10Fe-2.5Zr-1.5Mo	4.79	3.44	71.8	4.59	95.8	104.8		
Ti-10Fe-2.5Zr-3Mo	4.83	3.41	70.5	4.45	92.0	105.4		
Ti-10Fe-2.5Zr-2Sn	4.79	3.31	69.1	4.44	92.7	104.1		
Ti-10Fe-2.5Zr-4Sn	4.83	3.55	73.5	4.46	92.4	103.4		
Ti-10Fe-2.5Zr-2Cr_2C_3	4.78	3.16	66.1	4.38	91.6	105.2		
Ti-10Fe-2.5Zr-4Cr_2C_3	4.81	3.28	68.1	4.53	94.1	108.3	1.40	373
Ti-10Fe-2.5Zr-1.5Mn	4.78	3.19	66.7	4.32	90.4	101.4		
Ti-10Fe-2.5Zr-3Mn	4.81	3.19	66.3	4.37	90.9	103.7		

the microstructure of the sintered samples. Figure 6 shows the importance of vacuum level in Ti alloy sintering. Hardness and tensile tests were performed for each sample. The results show that as Fe and Zr increase, the theoretical density and mechanical properties increase, as listed in Table 6. The maximum properties of samples were obtained with the addition of 5Fe-5Zr wt % at 1,275ºC for 60 min.

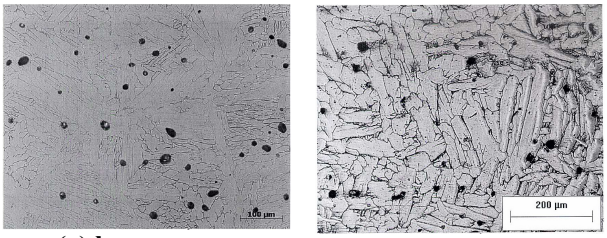

(a) low vacuum **(b) high vacuum**

Figure 6. SEM images of microstructures.

Table 6. Mechanical properties of Ti-Fe-Zr alloys.

Powder	Composition	Density (%)	Strength (MPa)	Elongation (%)	Vacuum (mtorr)
HDH	Pure Ti	91.8	643	3.13	10
	5Fe-2.5Zr	95.0	1025	3.54	
	5Fe-5Zr	94.0	1127	2.50	
Sponge	Pure Ti	94.8	524	4.52	0.3
	5Fe-2.5Zr	96.6	983	3.91	
	5Fe-5Zr	96.4	1067	3.20	

Evaluation of Boride Ti Alloys

As we proposed, the boride Ti alloy is one of the possible candidates for structural materials. We investigated the sintering behavior, the microstructure, and the mechanical properties of Ti-5Fe alloy with boron additions for structural applications, as shown in Figures 7 and 8. Samples were produced by mixing of initial pure metallic powders followed by uniaxial pressing with subsequent densification by sintering at 1,200°C

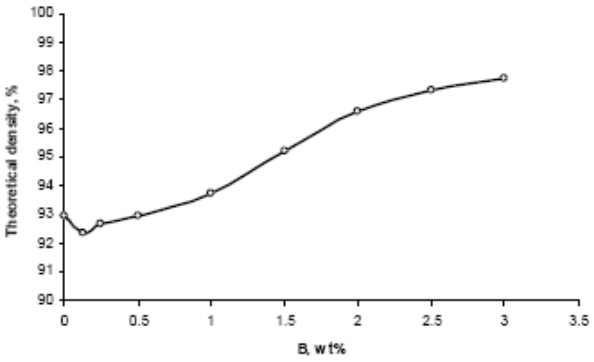

(a) density

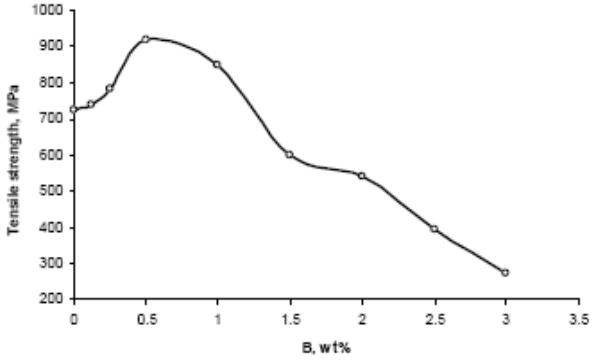

(b) tensile strength

Figure 7. Sintering behavior and mechanical properties of Ti-Fe alloys with boron additions.

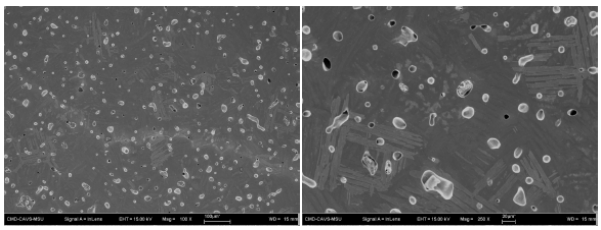

Figure 8. SEM images of Ti-5Fe-0.5CrB_2.

and 1,300°C, in vacuum. SEM was used to study the microstructures of the sintered samples. Hardness and tensile testing were performed for different samples. The results show that with increases of boron the theoretical density and tensile strength and hardness increase but the ductility decreases.

PIM Experiment

Initial trials on injection molding were conducted with the 17-4PH stainless steel feedstock that was readily available (Figure 9). We used a new binder formulation for sponge and HDH Ti powder

Figure 9. Molding trial by Ryer Feedstock (Stainless Steel).

injection molding to avoid formation of TiC as follows:

- 65 wt % paraffin wax,
- 25 wt % low density polypropylene,
- 9 wt % Fusabond,
- 1 wt % stearic acid, and
- 50 vol. % solid loading of –325 mesh Ti-HDH powder as determined by torque rheometer.

Modeling and Simulation

We first compared flow behavior of three different Ti powders, gas atomized, HDH, and spheroidized HDH Ti powders, as shown in Figure 10(a). We obtained the material properties from the literature on HDH Ti powder PIM for PIM simulation using donated PIMsolver, CetaTech, Inc. We selected the tensile specimen as the first geometry. We performed the first analysis simulation [Figure 10(b)], found possible processing windows [Figure 10(c)], and optimized the filling time for minimum injection pressure [Figure 10(d)].

Die Compaction

We obtained all material properties from a compressibility curve [Figure 11(a)] in the literature on commercial purity (CP) Ti powder for die compaction simulation using ABAQUS. We selected the gear as the first geometry. We performed the first analysis simulation [Figure 11(b)]. We have the optimization algorithm for loading schedule for uniform green compact density.

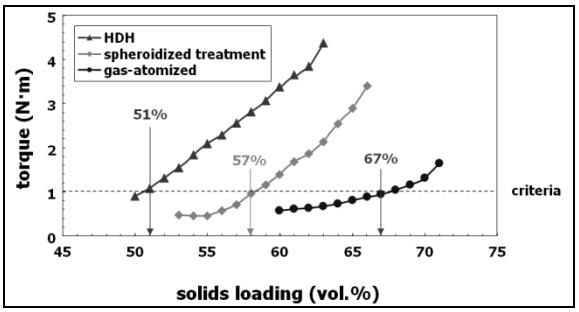

(a) Torque vs solid loading

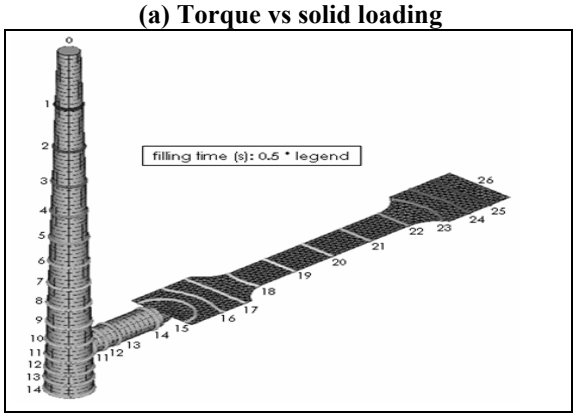

(b) Filling pattern

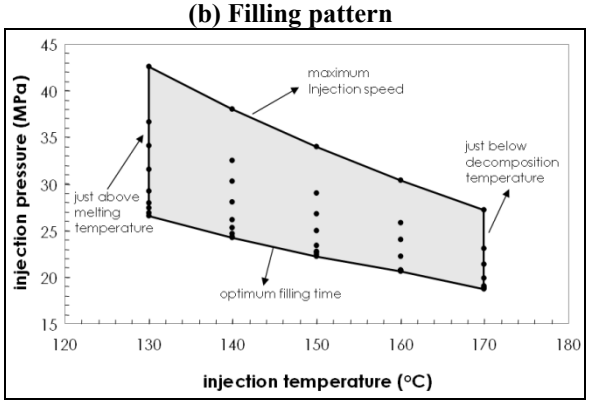

(c) Processing window

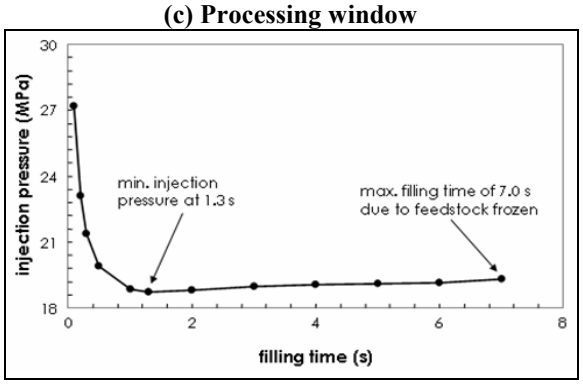

(d) Optimum filling time

Figure 10. The first trial of PIM simulation and optimization with HDH Ti powder.

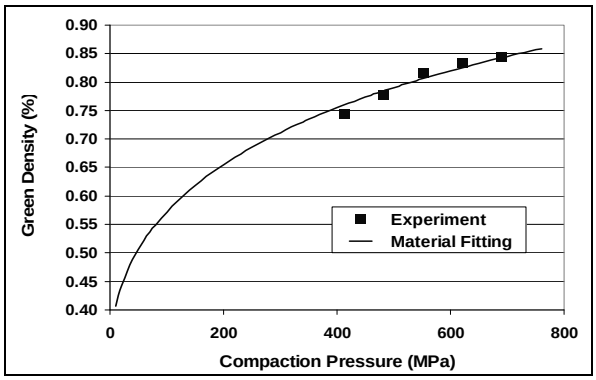

(a) Compressibility curve

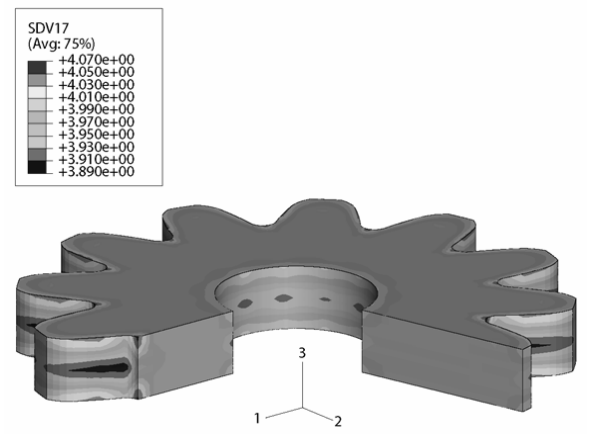

(b) Density distribution after compaction

Figure 11. The first trial of die compaction simulation with CP Ti powder.

Sintering and HIPing

We also have the capability to simulate sintering and HIPing processes. As for the HIPing, we obtained all material properties from creep test with pressure and temperature dependency of Ti-6Al-4V powder and performed simulation for powder and can. In addition, we also have developed the algorithm to optimize can geometry to obtain accurate final HIPed component dimension. But we could not find any Ti powder or Ti alloy powder material properties for simulations for the sintering in the literature.

Conclusions

In the last 6 months, we have accomplished the following:

- completed literature survey for low-cost Ti powder, Ti alloys for automotive application with cost analysis, and their processing techniques;
- designed and evaluated new Ti alloys including boride Ti alloy;
- performed PIM experiment; and
- developed simulation tool for PIM, die compaction, sintering, and HIPing, with some optimization.

Presentations/Publications/Patents

1. S. J. Park et al., "Rheological and Thermal Debinding Behaviors of Titanium Powder Injection Molding," *Metallurgical and Materials Transactions A*, 2008 (accepted).
2. O. Gulsoy et al., "Microstructure and Mechanical Properties of Sponge Ti and Its Alloy Powders with Various Powder Metallurgical Processes," *TMS 2008*, New Orleans, March 9–13, 2008.
3. O. Gulsoy et al., "Investigations on Novel Titanium Alloys for Structural Applications," *PM 2008*, Washington, D.C., June 8–12, 2008.
4. H. O. Gulsoy et al., "Effect of boron additions on microstructural and mechanical properties of Ti-5Fe alloy for structural applications," *5th International PM Conference*, Ankara, Turkey, October 8–12, 2008.
5. O. Gulsoy et al., "Development of Powder Injection Molding Process for Sponge Ti Alloy," *TMS 2009*, San Francisco, February 15–19, 2009.
6. O. Gulsoy et al., "Development of Powder Injection Molding Process for Sponge Ti Alloy," *PIM 2009*, Orlando, Florida, March 2–5, 2009.
7. Patents (in preparation): Three Ti alloy compositions.

C. Powder-Metal Performance Modeling of Automotive Components (AMD410*)

Project Manager: Howard Sanderow
Management & Engineering Technologies
4337 Oaks Shadow Drive
New Albany, OH 43054
(614) 775-0218; fax: (614) 775-0163; e-mail: metgroup@earthlink.net

Principal Investigator: Mark F. Horstemeyer (Paul T. Wang, Youssef Hammi)
Center for Advanced Vehicular Systems Chair in Solid Mechanics & Professor, Mechanical Engineering
Mississippi State University
206 Carpenter Bldg., P.O. Box ME
Mississippi State, MS 39762
(662) 325-7308; fax: (662) 325-7223; e-mail: mfhorst@me.msstate.edu

Russell Chernenkoff (retired from Ford Motor Company)
Metaldyne Sintered Component, Inc.
Metaldyne Powertrain Global Operations and Technical Center
47603 Halyard Drive
Plymouth, MI 48170
(734) 582-6227 ; fax: (734) 582-6250; email: russellchernenkoff@metaldyne.com

Paulo Rosa, Materials Development Engineer
Chrysler LLC
800 Chrysler Drive, CIMS 484-01-07
Auburn Hills, MI 48326
(248) 576-3197; fax: (248) 576-2177; e-mail: pr31@chrysler.com

Shekhar G. Wakade, Technical Specialist Materials Engineering
GM Powertrain
823 Joslyn Ave.
Pontiac, MI 48340
(248) 568-1143; fax: (248) 857-4425; e-mail: shekhar.g.wakade@gm.com

Glen Weber, Technical Specialist Engine Metals
Ford Motor Company
Building #1, Cube 12A037
Dearborn, MI
(313) 322-0175; e-mail: gweber@ford.com

Technology Area Development Manager: Joseph A. Carpenter
(202) 586-1022; fax: (202) 586-1600; e-mail: joseph.carpenter@ee.doe.gov

Field Project Officer: Aaron D. Yocum
(304) 285-4852; fax: (304) 285-4403; e-mail: aaron.yocum@netl.doe.gov

* Denotes project 410 of the Automotive Materials Division of the United States Automotive Materials Partnership, one of the formal consortia of the United States Council for Automotive Research set up by Chrysler, Ford, and General Motors to conduct joint, precompetitive research and development (see www.uscar.org).

Contractor: United States Automotive Materials Partnership (USAMP)
Contract No.: FC26-020R22910 through the DOE National Energy Technology Laboratory

Objective

- Our objective is to develop and experimentally validate math-based models for powder metallurgy component design and performance prediction. We will extend an existing USAMP microstructure-property model from casting to powder metallurgy (PM) for practical application in low strain-rate (design and durability) and high strain-rate (toughness-driven impact-strength) environments. We will use this model to evaluate and optimize an automotive component design (main bearing cap) as affected by materials (ferrous and non-ferrous) and manufacturing processes (compaction and sintering). We will implement this model into various software platforms such as ABAQUS [1]. This model will be robust enough to facilitate the insertion of various lightweight materials (such as aluminum and titanium) for future component applications.

Approach

- Determine current PM standards publications, component design guidelines, manufacturing, and evaluation methodologies. Provide a selection of metal powders that can satisfy design performance requirements, component design guidelines, and manufacturing and testing specifications across industry participants (Task 1).
- Evaluate and develop numerical modeling techniques to predict mechanical properties throughout PM component sections. The transition of current materials/design requirements to advanced structural PM components has created a need to predict the properties of components in all sections of design. In addition, the design processes should consider the least-cost, lowest-mass product designs and reduced development lead-time. We will extend an existing math-based framework with the abilities to predict PM component structures and properties accurately throughout the compaction and sintering processes (section size, density variation, dimensional tolerances, potential for cracking), and with the input of alloys and process parameters (machine functions, tool and powder temperatures, friction and pressure). We will capture the history of a PM part through its pressing, sintering, and life-cycle performance using the developed multiscale methodology. (Task 2).
- Develop component- and vehicle-level testing to validate durability, quality control and performance of PM parts. We will determine quality control process factors (powder properties, press settings, tooling design, and furnace conditions) for PM parts production in terms of their impact on process variations and quality improvement. We will use optimization and statistical techniques to help determine the main factors affecting the final component. We will perform validation experiments considering actual boundary conditions from real processes to fracture the components. (Task 3).
- Manage and report program activities. We will incorporate bi-weekly teleconferences, have two technical review sessions per year and have intermittent meetings throughout the year to report progress and discuss issues. Proper execution of this task will greatly enhance the visibility and the value of this program. Reports generated from this program will follow the guidelines suggested by the Department of Energy (DOE) and United States Council for Automotive Research (USCAR). (Task 4).
- Perform Technology/Commercial transfer throughout the product value chain. To date, there exists limited accountability for major research and development (R&D)/technical institutions to foster the infrastructure to support large-scale applications of PM components. If the auto industry wishes to take advantage of PM's potential weight and cost reduction opportunities, they must nurture PM development through programs sponsored and directed by USCAR. The project team will request the professional support of societies to publish notices of meetings and project information, as released by the project team. (Task 5).

Accomplishments

- Determined the cap eccentricity parameter to complete the powder characterization (represented by a p-q plot) of FC-0205 Ancorsteel powder provided by Hoeganaes and 205Q powders provided by Metaldyne. (Task 2).
- Measured the density distributions of the green and sintered main bearing caps provided by Metaldyne using Immersion Density and Image Analysis. Measured the density distribution of the sintered main bearing cap (MBC) using two-dimensional (2D) X-Ray Computed Tomography. (Task 3).
- Performed springback analysis of the MBC after compaction to measure the dimensional changes and to determine the density distribution out of the die. (Task 2).
- Performed experiments on notched Bridgman specimens to determine the damage at failure using computed tomography. (Task 3).
- Performed an MBC monotonic performance test (loaded to failure) to determine the tensile strength and failure location of the MBC. (Task 3).
- Validated the plasticity/fatigue model on the MBC with the information provided by Metaldyne. (Task 3).
- Performed sensitivity and uncertainty analysis to identify which input parameter contributes more to the overall uncertainty in the compaction model. (Task3).
- Submitted three conference papers at Metal Powder Industries Federation Powder Metal 2008 Conference (MPIF-PM2008). (Task 4).
- Developed several software programs with graphical interfaces to calibrate the model constants for compaction, sintering, performance and fatigue. (Task 4).
- Held a Technology Transfer Training Session for PM end users at Ford Research Laboratory, Dearborn, MI. (Task 4).
- Used the model to optimize the compaction process for a MBC. (Task 4).
- Completed the 2008 semi-annual and annual reports for release to USCAR and DOE. (Task 4).

Work Plan for Remainder of the Project

- Perform sintering analysis of the MBC for the FC-0205 and 205Q powders using experimental data and for an Al alloy using literature data. (January, 2009)
- Correlate the FC-0205 and 205Q sintering data with the models. (January, 2009)
- Validate the sintering simulation results with the experimental results on the MBC. (January, 2009)
- Apply the modeling to lightweight material such aluminum powder using literature data and predict the performance and fatigue property in a MBC. (January, 2009)
- Perform optimization simulations of the MBC. (January, 2009)

Introduction

The objective of this project is to develop and experimentally validate math-based models for powder metallurgy component design and performance prediction.

During the last twelve months, the remaining closed-die compaction tests were conducted on the FC-0205 and 205Q powders to determine the cap eccentricity parameter, which was optimized to determine the shape of the yield surface during powder densification. The completed compaction data were used to generate p-q plots, which define the density value for any stress state and graphically represent the yield surface evolution during compaction. An uncertainty analysis was performed to quantify the overall uncertainty of the outputs due to uncertainties in the input parameters. To identify which input parameter's uncertainty contributes more to the overall

uncertainty, a sensitivity analysis was also conducted.

Regarding the model development, the springback analysis has been performed on the MBC to determine the density distribution out of the die. The density distribution after springback was used as the initial state for the sintering model, as well as the initial state for the performance and fatigue analysis because the density variation during sintering is almost insignificant for steel-based powders.

Performance tests have also been completed for notched Bridgman and MBC samples to determine the damage failure of the sintered MBC under monotonic loading. The performance model material constants were validated by comparing the plastic and damage prediction of the Bridgman notch tensile specimens to the experimental results. A finite-element analysis (FEA) simulation of the monotonic testing of the MBC was completed and validated with the experimental test results.

As such the model correlation and validation for the life cycle analysis will take the information from the after compacted and after sintered processes. The fatigue failure and life was determined using the multistage fatigue (MSF) model developed at the Center for Advanced Vehicular Systems (CAVS).

A preliminary design optimization study was conducted on the MBC to improve density distribution and increase mechanical properties. Some results from this study are included. The compaction model implementation for aluminum MBC was also completed and the results presented.

Finally, several software programs have been developed at CAVS to provide the PM end users a graphical interface for calibrating the model parameters for the compaction, sintering, performance and fatigue processes. This software, along with the experimental and computational work, was presented to PM end users during a technology transfer session in May, 2008.

Powder Characterization

A number of experimental tests were performed to gather the data necessary for characterization and validation of the constitutive equations of the compaction and sintering processes.

To determine the cap eccentricity parameter in the Modified Drucker/Prager Cap Model [2], closed-die compaction tests were performed on cylindrical samples. Compaction tests were performed on several FC-0205 powder cylinders of 0.5-inch diameter with four different fill depths. The cap eccentricity parameter, R, which can be derived from the ratio of axial and radial stresses, was determined with an inverse method by comparing the numerical hoop strains to the measured hoop strains at different location on the die. The radial stress, exerted by the powder on the die wall, was calibrated by modifying the cap eccentricity parameter R in order to fit the strain gage with the highest hoop strain.

By combining the cap eccentricity results with the previous Brazilian, compression and compressibility test results, the failure line and cap surface at different densities were determined. Figure 1 shows the equidensity lines in the hydrostatic pressure (p)—von Mises (q) stress space for the FC-0205 and 205Q powders, which correspond to the evolution of the Modified Drucker/Prager compaction model during densification.

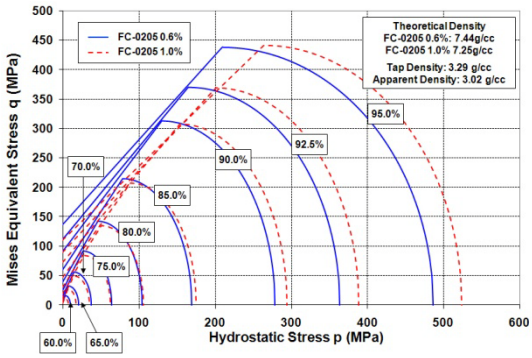

Figure 1. Isodensity curves in the p-q plane representing the evolution of the Cap Model with respect to relative density (% theoretical).

Sensitivity and Uncertainty Analysis

Sensitivity analysis aims to identify which input parameter, such as initial density ρ0, maximum plastic volumetric strain W, or material parameters c1, c2, d1, d2, ρd, R1, R2, ρc and k, contributes more to the overall uncertainty. In the compaction model, we obtain the sensitivities by simply computing the derivatives of the output variables, namely the green density, the interparticle friction, the material cohesion, the cap eccentricity, and the elastic modulus.

Figure 2 shows the sensitivity of the compressibility curve for FC-0205 with 0.6% wax. For all of the output variables, we notice that the most dominant parameter is the initial (or tap) density.

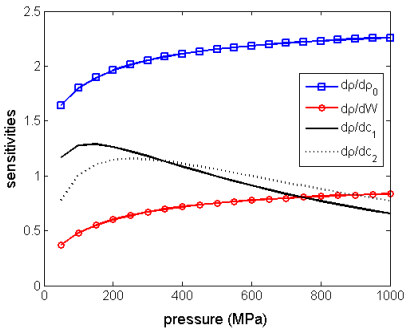

Figure 2. Sensitivity of compressibility curve for FC-0205 with 0.6% Acrawax.

Uncertainty analysis quantifies the overall uncertainty of the output due to uncertainties in the input parameter. To quantify the effect of uncertainties on the material constitutive model, we use uncertainty propagation based on first order Taylor series expansion [3] as given in Eq. (1):

$$VAR(Y) = \sum_{i=1}^{N} \left(\frac{dY}{dX_i} \right)^2 VAR(X_i) \quad , \qquad (1)$$

where *VAR* stands for variance (a measure of uncertainty, square of standard deviation), X_i is the ith input uncertainty, N is the number of uncertain input variables and Y is the output. Since the analytical formulations exist, the uncertainty analysis is computationally inexpensive. If the analytical formulation did not exist and the output parameter calculations were expensive, then we would perform the uncertainty analysis using more efficient techniques {e.g., Dimension Reduction (DR) method + Extended Generalized Lambda Distributions (EGLDs) technique proposed by Acar et al. [4]}.

Figure 3 shows that the most of the FC-0205 material test data falls between the 95% confidence bounds. Notice that the uncertainty in the compressibility curve reduces as the pressure is increased.

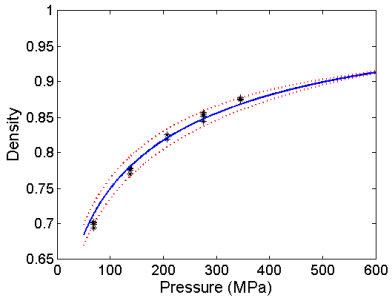

Figure 3. Uncertainty in the compression curve for FC-0205 with 0.6% Acrawax.

Figure 4 depicts the variation of uncertainties in the interparticle friction of FC-0205 as the green density changes. We notice that the effect of the input uncertainties on the interparticle friction is more profound when 1.0% Acrawax is used in the powder. Identically, the increase of the wax in the powder from 0.6% to 1.0% results in a huge uncertainty in the material cohesion.

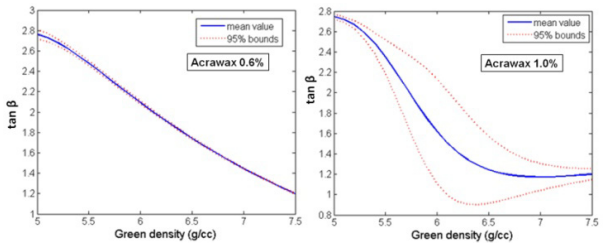

Figure 4. Uncertainty in the interparticle friction for FC-0205 with different Acrawax amounts.

The reason for the significant difference between the results of powder with 0.6% and 1.0% acrawax is due to the higher scattering of failure stress data points in the compression tests of the FC-0205 1.0% Acrawax.

Compaction Modeling

Springback Analysis

Ejection is an important part of the compaction process because it determines the final shape of the unloaded part, with or without cracks. Due to three-dimensional contact nonlinearities between the powder and tools that lead to convergence issues in ABAQUS/Standard, the ejection results presented were obtained by simply removing the tools from the compacted powder to obtain the dimensional and density changes after springback.

For the springback analysis, the material solution of the compacted model (without the tools) was exported from ABAQUS/Explicit, and the appropriate boundary conditions were applied. In this simulation, no further powder densification was considered and the powder compact was assumed elastic at any material point. During the springback analysis, it was calculated that the volume grew approximately 0.6% with most of the dimensional changes occurring along the compacting direction. These results are consistent with the non-uniform density measured in the real PM component after compaction.

Performance Testing and Modeling

Notch Bridgman Test

Monotonic loading of notch Bridgman specimens was performed up to failure. The use of the notch geometry creates stress triaxiality gradients in the specimens allowing for both experimental and numerical methods to be validated. Two different notch radii are chosen for the analysis and labeled as R60 and R150 for notch radii of $R = 0.060$ in and $R = 0.150$ in, respectively. By analyzing the tested Bridgman specimens we studied how different triaxiality conditions influence the damage behavior of the material. Strain-controlled experiments on the notch Bridgman specimens were performed to failure and to 98%, 95%, and 90% of the failure load using an Instron 5882 testing machine with a $\pm$100 kN maximum loading capacity. After testing, the damage in the specimen was analyzed. Results from the tests for the Bridgman specimens revealed that the larger notch root radius exhibited more plasticity than the smaller radius specimens.

Notch Test Validation

The performance model material constants were validated by comparing the plastic and damage behavior of the material with the Bridgman notch tensile specimens to the experimental results. The ratio between one half of the cross-sectional diameter of the specimen at the centre of the notch, a, respect to the notch radius, r. Therefore, R60 has a ratio a/r=0.142/0.06 =2.367 and for R150, a/r=0.142/ 0.075=1.893. Figure 5 presents a comparison between the load- displacement curves obtained experimentally and computationally using the FEA model.

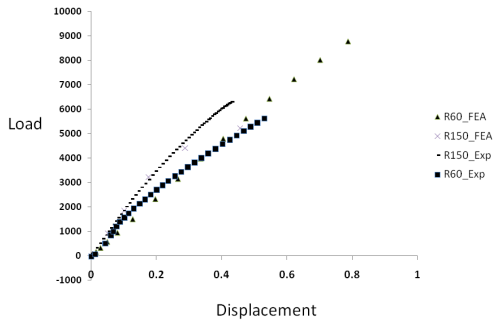

Figure 5. Load displacement comparison for notch Bidgman specimens of the experiment and FEA results.

The model predicts the maximum load and fracture displacement for the R60 specimens. All modeled curves show a very slight variation in the elastic slope, while in the experiments the variation is more noticeable. The stress-strain curves take into account the initial cross-sectional area of the specimen, as well as the area reduction after passing the ultimate strength point. In comparison, the load-displacement plots only reflect the displacement applied to the specimen at certain load. The model predicts satisfactorily the elongation at fracture for the R60 and R150. Damage levels are directly proportional to triaxiality magnitude. Thus, larger levels of triaxiality will not only translate in a greater area where the voids nucleate and evolve, but also these voids will have a larger fracture diameter.

MBC Performance Tests

The tensile strength of a sintered MBC was determined experimentally for validation of the internal state variable (ISV) plasticity-damage

model developed for powder metallurgy materials. The load was applied on both legs of the bearing cap as indicated in Figure 6.

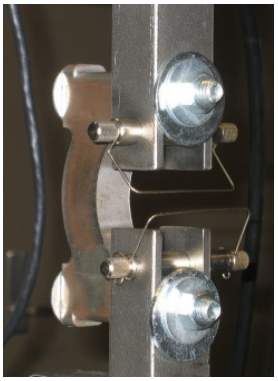

Figure 6. Test fixture and loading application of the MBC.

Initial tests based on strain control indicated some plasticity occurring in the region of test fixture component that connects through the bolt holes of the MBC. Therefore, subsequent tests based on displacement control were performed using a test fixture of a higher stiffness. The MBCs were tested on a 20 kip MTS load frame at a rate of 0.25 mm/s and at room temperature (~273 K) in laboratory air with relative humidity (RH) near 45–60. The MBCs were preloaded to 30 lbf, which ensures the load is applied at the end of the bearing caps. Programming the test, controlling the experiment, and collecting data were performed by using the MTS controller application, Multipurpose Test Ware (MPT). Data acquisition was recorded every 100 ms by MPT with extension, load, and displacement recorded.

The load-displacement data for the monotonic tensile tests of the MBCs is reported in Figure 7. The failure location was basically the same for all the MBCs tested and agrees favorably with test results by Metaldyne [5].

MBC Performance Test Validation

A finite element model for the monotonic load testing of the bearing cap was developed to study the damage state of the bearing cap. Using ISV theory, damage-dependent material parameters are used to capture the location of failure. The material parameters are obtained from the

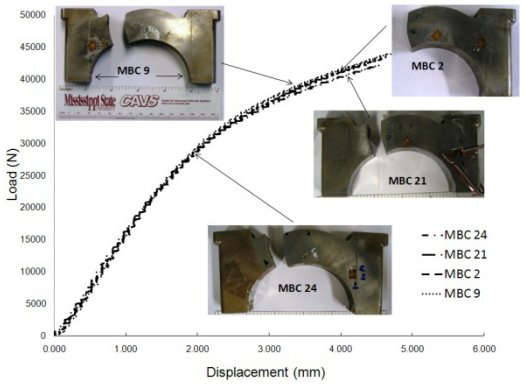

Figure 7. Experimental load-displacement results for MBC and corresponding fractured MBCs.

experimental data and applied to the Bammann-Chiesa-Johnson (BCJ) ISV model. Figure 8 provides a comparison of the FEA simulation results of the monotonic testing with the experimental results. The comparison indicates that the FEA results were very close to those of the experimental results when comparing the strains measured from applied strain gages in the region noted.

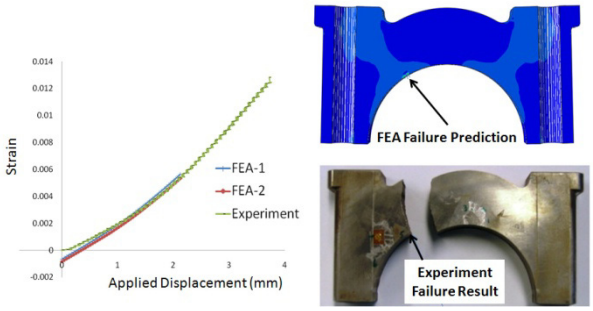

Figure 8. Comparison of strain-displacement results for the FEA model and the experiment test results for the MBC.

Figure 8 shows that the model predicted the exact location where damage initiated in the MBC and not where the greatest von Mises stress existed, as shown in Figure 9. The reason the classical Mises stress does not correctly capture the damage is because it does not account for the heterogeneities arising from the porosity distribution and because damage nucleates, grows, and coalesces more with the stress triaxiality. As discussed previously, the proposed ISV plasticity-damage model captures this effect and therefore correctly predicts the failure location.

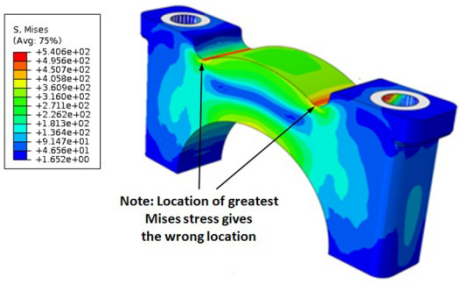

Figure 9. Mises stress distribution for the MBC after performance testing.

Fatigue Modeling

The fatigue analysis is performed on the MBC by modeling the Metaldyne experimental fatigue fixture. A cyclic sine waveform loading was applied onto a shaft, which is connected to the MBC through a half-circular ring. Different maximum loads, from 20,000 to 23,000 lbs, were tested up to 10 million cycles, with a minimum load of 1,000 lbs. The lower and upper bounds of the fatigue life were determined from strain-controlled, low-cycle fatigue tests on samples of, respectively, high and low porosities (Figure 10). The MSF model was applied to predict the fatigue life of the MBC in the FEA [6,7]. Using the fatigue software MSFfit, developed at CAVS, the fatigue parameters were calibrated on the low-cycle fatigue curve and on its extrapolation for the high-cycle regime. The MSF model was implemented into the user subroutine UVARM to generate element output within ABAQUS/Standard.

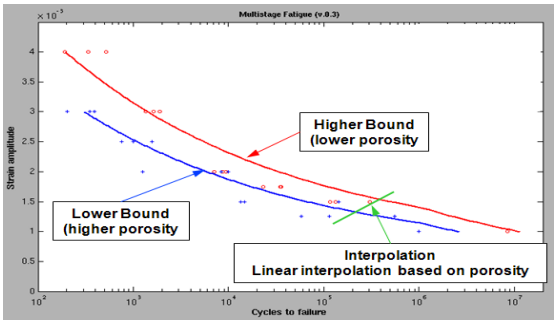

Figure 10. Strain Amplitude vs. Cycle to failure curve for the lower and higher bounds.

Multistage Fatigue (MSF) Model

The MSF approach decomposes fatigue life into four consecutive stages based on the microstructural details of fatigue crack growth based upon, i.e.,

$$N_{Total} = N_{Inc} + N_{MSC} + N_{PSC} + N_{LC} = N_{Inc} + N_{MSC/PSC} + N_{LC} \quad , \qquad (2)$$

where N_{Total} is the total fatigue life. Here, N_{Inc} is the number of cycles to incubate a crack at a micronotch; N_{MSC} is the number of cycles required for propagation of a Micro-structurally Small Crack (MSC); N_{PSC} is the number of cycles required for propagation of a physically small crack (PSC), during the transition from MSC status to that of a dominant long crack (LC). In Equation (2), for simplicity the MSC and PSC regimes are combined into one mathematical form. The number of cycles required for LC propagation is given by N_{LC}, applicable to growth in the range $a >$ 200-800 µm, where a is the crack length, and the crack propagation depends on the amplitude of loading and the corresponding extent of microplasticity ahead of the crack tip.

Fatigue Analysis

The density distribution was mapped from the PM process analysis to define the elastic mechanical properties for each material point of elements. Because the stresses throughout the MBC are within the elastic domain, the MBC is defined by density-dependent elastic properties only. Figure 11 shows the effective strain amplitude Δε

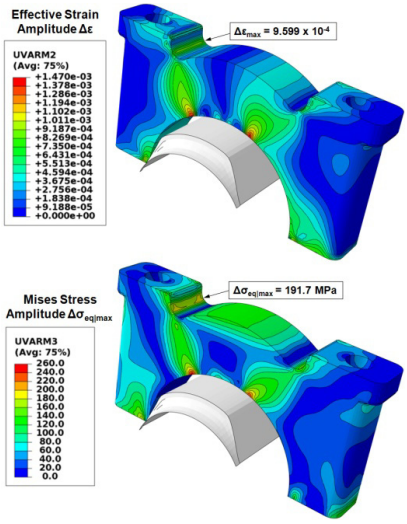

Figure 11. Effective strain and Mises stress amplitudes for a shaft load of 23,000 lb.

and Mises stress amplitude $\Delta\sigma_{eq}$ that are considered in the fatigue model.

The fatigue lives N_{Inc}, N_{SC}, N_{LC} and N_{Total} were calculated using the interpolation based on density of either the fatigue parameters (Interpolation I) or the fatigue lives (Interpolation II) of the lower and upper bounds (Figure 10). The fatigue life N_{Total} is predicted to be near 7.2 million cycles at the location shown on Figure 12 for a shaft load of 23,000 lbs. Low values of N_{Total} around the arch were ignored due to the fact that the contact nodes leads to a certain strain localization.

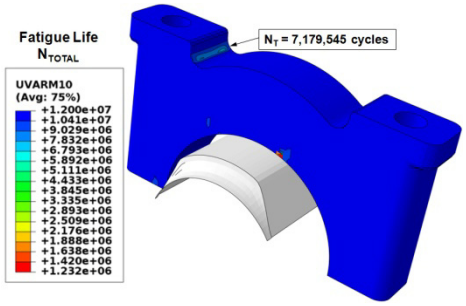

Figure 12. Fatigue life N_{Total} and its location for a shaft load of 23,000 lb.

Table 1 shows the fatigue lives for different shaft loads. Only the solution with heterogeneous density was able to capture the correct prediction. The fatigue test is considered to be successful when the fatigue life is greater than 10 million cycles.

Compaction Modeling for Al MBC

To evaluate material substitution and lightweight materials in the MBC parts, the compaction modeling of a MBC was performed with aluminum material parameters that were calibrated using literature data [8]. The simulation was performed using the exact same tool geometries and motions as the FC-0205 MBC. The density distribution shows the same pattern as for the steel MBC (Figure 13) but the density values are quantitatively much lighter.

Table 1. Fatigue lives for Interpolation I and II at different shaft loads

Higher Bound (Low Homogeneous Porosity)				
Fatigue Life	Shaft Loading (lbs)			
	20,000	21,000	22,000	23,000
N_{INC}	> 10,000,000	> 10,000,000	> 10,000,000	> 10,000,000
N_{SC}	2	2	2	1
N_{LC}	142,942	106,044	79,826	60,890
N_{TOTAL}	> 10,142,944	> 10,106,046	> 10,079,828	> 10,060,891
Failure	PASS	PASS	PASS	PASS

Lower Bound (High Homogeneous Porosity)				
Fatigue Life	Shaft Loading (lbs)			
	20,000	21,000	22,000	23,000
N_{INC}	2,399,554	1,658,665	1,176,098	778,410
N_{SC}	1	1	1	1
N_{LC}	173,956	129,105	97,223	74,187
N_{TOTAL}	2,573,511	1,787,771	1,273,322	852,598
Failure	FAIL	FAIL	FAIL	FAIL

Interpolation I (Heterogeneous Porosity)				
Fatigue Life	Shaft Loading (lbs)			
	20,000	21,000	22,000	23,000
N_{INC}	> 10,000,000	9,902,806	8,341,563	7,109,965
N_{SC}	1	1	1	1
N_{LC}	163,212	121,115	91,194	69,579
N_{TOTAL}	> 10,163,213	10,023,922	8,432,758	7,179,545
Failure	PASS	CRACK	FAIL	FAIL

Interpolation II (Heterogeneous Porosity)				
Fatigue Life	Shaft Loading (lbs)			
	20,000	21,000	22,000	23,000
N_{INC}	> 10,000,000	> 10,000,000	8,553,476	7,485,101
N_{SC}	1	1	1	1
N_{LC}	163,212	121,115	91,194	69,579
N_{TOTAL}	> 10,163,213	> 10,121,116	8,644,671	7,554,681
Failure	PASS	PASS	FAIL	FAIL

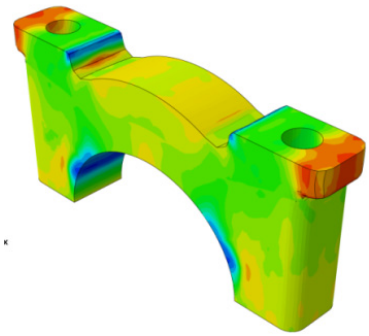

Figure 13. Density distribution for an Al-MBC.

Technology Transfer

Several software programs have been developed at CAVS to provide the PM end users a graphical interface for calibrating the model parameters for the compaction, sintering, performance and fatigue processes.

The software utility for the Modified Drucker-Prager Cap model was developed using experimental data (compressibility, material cohesion, interparticle friction, cap eccentricity, Young's modulus and p-q data) to calibrate the model constants. The software allows the influence of each constant on the P-Q plot to be interactively investigated.

A software utility for calibrating the master sintering curve from dilatometry data was also developed. The software utility for the performance and fatigue processes will be made available to the PM end users after additional verification procedures are completed.

Conclusions

For the Powder-Metal Performance Modeling of Automotive Components project, determination of the microstructure-property relations and parameter calibration was completed for compaction model. The ejection feature represented by a springback analysis was performed on a MBC, giving the initial density distribution that was used for the preliminary fatigue fixture analysis of the MBC. Model simulation of the fatigue failure and life of the MBC were also evaluated and validated based on favorable comparison to the experimental test results. These results will be considered for better design, performance and mass optimization. Regarding the sintering model, additional dilatometer tests were performed to measure the dimensional changes of green compacts that have relatively the same green density as the green MBC. Finally, the compaction and sintering property database on aluminum was collected from another DOE project in order to evaluate material substitution and lightweight materials in the MBC parts, and the compaction model prediction was presented.

Publications

1. P. Allison, M. Horstemeyer, Y. Hammi, and H. Brown. 2008, "Stress-State Dependence of FC-0205 Steel Powder," MPIF/APMI 2008 World Congress on Powder Metallurgy & Particulate Materials, June 8–12, Washington, D.C.
2. Y. Hammi, T, Stone, L. Arias-Meza, P. Allison, and M. Horstemeyer. 2008, "Modeling for Powder Metallurgy Component Design and Performance Prediction," MPIF/APMI 2008 World Congress on Powder Metallurgy & Particulate Materials, June 8–12, Washington, D.C.
3. T. W. Stone, L. Arias-Meza, T. N. Williams, Y. Hammi, H. El Kadiri, and M. Horstemeyer. 2008, "Comparison of Density Measurement Techniques for Large PM Components," MPIF/APMI 2008 World Congress on Powder Metallurgy & Particulate Materials, June 8–12, Washington, D.C.

Acknowledgements

The authors would like to acknowledge funding from the Center for Advanced Vehicular Systems at Mississippi State University and from USAMP Advanced Materials Division (AMD) 410. We thank Michael O'Neill, Ernie Bertolasio and Edmund Ilia from Metaldyne Sintered Components for all the information and material samples they provided us.

References

1. Abaqus, User's Manual, Version 6.7, Hibbit, Karson & Sorensen, Inc., 2006.
2. O. Coube and H. Riedel. 2000, "Numerical Simulation of Metal Powder Die Compaction with Special Consideration of Cracking", Powder Metallurgy, Vol. 43, No. 2, pp. 123–131.
3. H. S. Ang and W. H. Tang. 2006, "Probability Concepts in Engineering: Emphasis on Applications to Civil and Environmental Engineering," 2nd Edition, Wiley.
4. E. Acar et al. 2008, "Uncertainty analysis of damage evolution computed through microstructure property relations," Proceedings of the ASME IDETC/CIE 2008, August 3–6, New York City, New York, USA.
5. E. Ilia et al. 2003, "Development of a Main Bearing Cap For an Inline 6 Cylinder Engine," Proceedings of the 2003 International Conference on Powder Metallurgy &

Particulate Materials, June 8–12, Las Vegas, NV, USA.

6. D. L. McDowell et al. "Microstructure-Based Fatigue Modeling of Cast A356-T6 Alloy," Engineering Fracture Mechanics, Vol. 70, pp. 49–80, 2003.
7. Y. Xue et al. 2007, "Microstructure-based multistage fatigue modeling of a 7075-T651 aluminum alloy," Engineering Fracture Mechanics, Vol. 74, pp. 2810–2823.
8. S. C. Lee and K. T. Kim. 2002, "Densification behavior of aluminum alloy powder under cold compaction", International Journal of Mechanical Sciences, Vol. 44, pp. 1295–1308.

D. Examining Fundamental Mechanisms of Tooling Wear for Powder Processing

Principal Investigator: Seong Jin Park
Associate Research Professor
Center for Advanced Vehicular Systems, 2215
Mississippi State University, P.O. Box 5405
Mississippi State, MS 39762-5405
(662) 325-8565; fax: (662) 324-4001; e-mail: sjpark@cavs.msstate.edu

Co-Principal Investigator: Youssef Hammi
Center for Advanced Vehicular Systems
Mississippi State University, P.O. Box 5405
Mississippi State, MS 39762-5405
(662) 325-5452; e-mail: yhammi@cavs.msstate.edu

Co-Principal Investigator: Haitham El Kadiri
Assistant Research Professor
Center for Advanced Vehicular Systems
Mississippi State University, P.O. Box 5405
Mississippi State, MS 39762-5405
(662) 325-5568; fax: (662) 617-4790; e-mail: elkadiri@cavs.msstate.edu

Co-Principal Investigator: Paul T. Wang
Manager, Computational Manufacturing and Design
Center for Advanced Vehicular Systems
Mississippi State University, P.O. Box 5405
Mississippi State, MS 39762-5405
(662) 325-2890; fax: (662) 325-5433; e-mail: pwang@cavs.msstate.edu

Co-Principal Investigator: Anthony Antonyraj
Assistant Research Professor of Materials Science
Center for Advanced Vehicular Systems
Mississippi State University, P.O. Box 5405
Mississippi State, MS 39762-5405
(662) 325-8558; email: aanton@cavs.msstate.edu

Technology Area Development Manager: Joseph A. Carpenter
(202) 586-1022; fax: (202) 586-1600; e-mail: joseph.carpenter@ee.doe.gov

Field Project Officer: Aaron D. Yocum
(304) 285-4852; fax: (304) 285-4403; e-mail: aaron.yocum@netl.doe.gov

---

Contractor: Mississippi State University (MSST)
Contract No.: 4000054701 through the National Energy Technology Laboratory

---

Objective

- Develop an innovative design of tooling surfaces and novel lubricants for processing ferrous and lightweight materials.

Approach

- Productivity and performance of powder metallurgy (P/M) parts rely on the behavior of a surface oxide, which by nature is a dispersion-strengthened product. This work plans to use coated powders to provide an opportunity to control tool friction, surface reactions, and component strength. This research will apply new tools to the old problem of aluminum P/M. It relies on powder changes, alloying and processing optimization to produce nearly full-density products with complex shapes and dimensional precision. The work is fundamentally new, since very little efforts have been focused on moving forward the lightweight automotive components fabricated by P/M for meeting desirable property levels, as comparable with traditional ferrous P/M. Significant progress is expected in the key areas, such as the optimal particle size distribution, powder coatings, active lubricants, and computer simulations.

Accomplishments

- Developed a new methodology to quantify tool wear for die compaction in the mold using silicon rubber.
- Proposed a new integral equation to quantify tool wear from numerical simulation results.
- Characterized the effect of lubricant on tool wear.
- Obtained industry sponsor in-kind support, including CetaTech and CM Furnaces.
- Published six journal papers and eleven conference papers related to this task.
- Produced two students with Master degree through this task.
- Worked with Oak Ridge National Laboratory (ORNL) wear test facility, through the High Temperature Materials Laboratory (HTML)/ORNL user program
- Developed full design and optimization algorithms

Introduction

P/M techniques are widely used to fabricate complex automotive components from ferrous powders. The energy efficiency and cost attributes of P/M are recognized by the domestic automotive industry. With the push for lighter-weight, higher-strength and more- durable structures, the barriers to lightweight P/M in domestic automobiles needs to be addressed. Besides economics, the technical barriers are: tool wear, performance and ductility at high strain rates (related to crashworthiness). In this work, we use aluminum (Al) powders to demonstrate the development of tooling wear control technology. Similar methodology could be applied to other lightweight powders such as titanium (Ti).

Current Progress Based on Schedule Planned

Table 1 shows the current progress based on the schedule planned. All subtasks have been accomplished, and the final report is presented here.

Table 1. The proposed project schedule with marks of progresses.

Subtasks	Year 1				Year 2			
	Q1	Q2	Q3	Q4	Q1	Q2	Q3	Q4
5.1 Perform thorough literature review to strengthen the quantitative goals in terms of materials and processes	100							
5.2 Create first FEM simulations to establish a context for the research	100							
5.3 Design Experiment in terms of Al powders, additives, lubricant for tool wear and high strength alloy	100							
5.4 Perform compaction and sintering trials to evaluate whole processes with new alloys		100						
5.5 Develop experimental techniques for quantifying tool wear		100						
5.6 Develop a constitutive relation for tool and FEM simulation tool					100			
5.7 Perform mechanical testing including tensile test, three-point bending, and hardness					100			
5.8 Perform microstructure evaluation by SEM testing of the final sintered product and fracture surface analysis						100		
5.9 Employ computer simulations to optimize learning and rapidly advance research						100		

Summary of the Progress

This project (referred to as Task 5 within the MSST lightweighting materials projects) comprises three research categories: die-wear measurement, aluminum-alloy evaluation, and modeling and simulation for tool wear.

Characterization Tool Surface Quality

We established a new methodology to quantify tool wear during die compaction (Figure 1a) through a nondestructive method using RepliSet

(Figure 1b) and a TalySurf profilometer (Figure 1c).

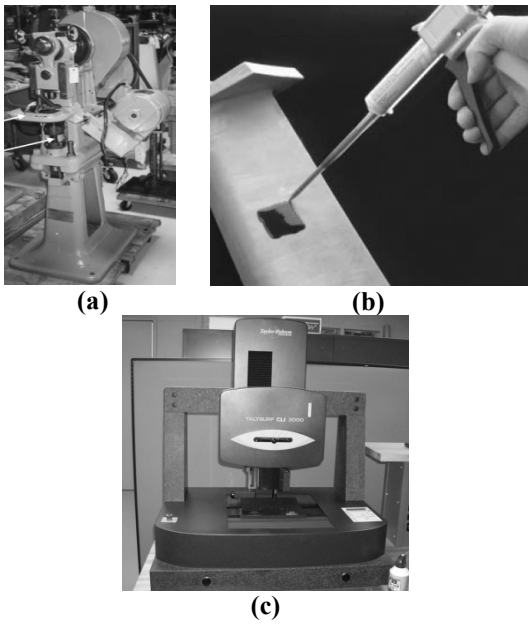

Figure 1. Establishment of new methodology to quantify tool wear: (a) compaction machine with die for wear measurement, (b) RepliSet (silicon rubber and shot gun) and (c) TalySurf profilometer for surface measurement.

Once the methodology was set up, we calibrated a silicon rubber technique and found that its resolution was ±0.5 μm. We measured tool wear with three die-tool materials and four different powders including die diameter, die weight, surface roughness and so on for quantifying tool wear. In addition, the microstructure was evaluated using scanning electron microscopy (SEM), as shown in Figure 2.

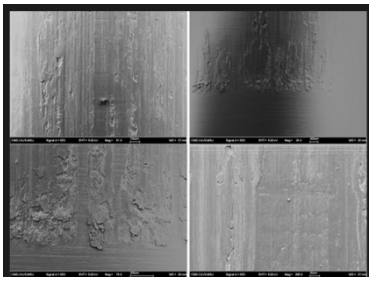

Figure 2. SEM image of silicon rubber surface to investigate ability of transcription of RepliSet.

Tribological Measurement for Tool Wear

By collaborating with ORNL, tribological experiments were designed to obtain specific material properties within minimized time and cost. In this study, two methods (1) a modified pin-on-flat test and (2) a continuous-loop abrasion test, were employed to observe wear occurring on die materials, as shown in Figure 3. Figure 4 shows microscopic images from these tribological

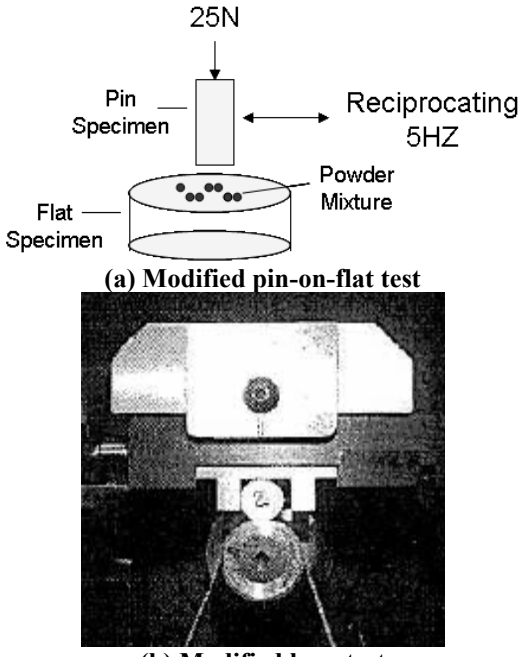

Figure 3. Tribological experiments.

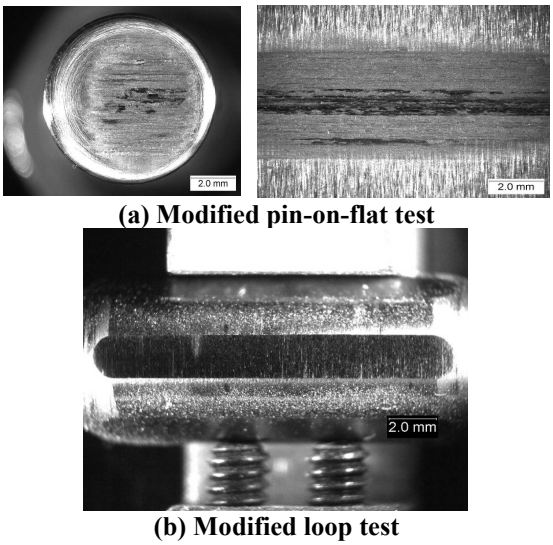

Figure 4. Microscopic images from tribological experiments.

experiments. The quantification of wear was based on the mass-loss measurement, dimensional-change measurement, and dimensional-change calculation. From these measurement results, we obtained *k* values for Archards' Law of wear as shown in Figure 5, which was used for finite-element model (FEM) simulations.

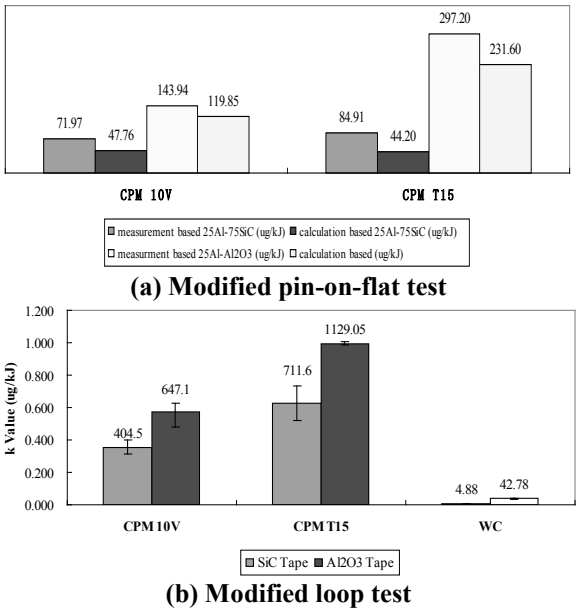

Figure 5. *k* values for Archards' Law of wear from tribological experiments.

Automatic Compaction Experiment for Tool Wear

Automatic compaction was used to simulate the industrial production process. To observe the effect of wear of the Al-SiC and Al-Al_2O_3 powder mixtures on tooling in an industrial environment, a table-size press was used with a tungsten carbide BC-14S die, while top and bottom punches were made from M4 tool steel. Cylindrical compacts with a diameter of 6.35 mm and a height of approximately 4.5 mm were compacted at a rate of approximately 70 compacts per minute. The bottom punch was adjusted to hold a filling height of 7.8 mm. The upper punch stroke length was calibrated to achieve green compact relative densities of 80% theoretical. For each of the powder mixture compositions, 30,000 samples were compacted. We then evaluated the effects of the amount of hard additives, the number of operations, and the amount of lubricants as shown in Figure 6.

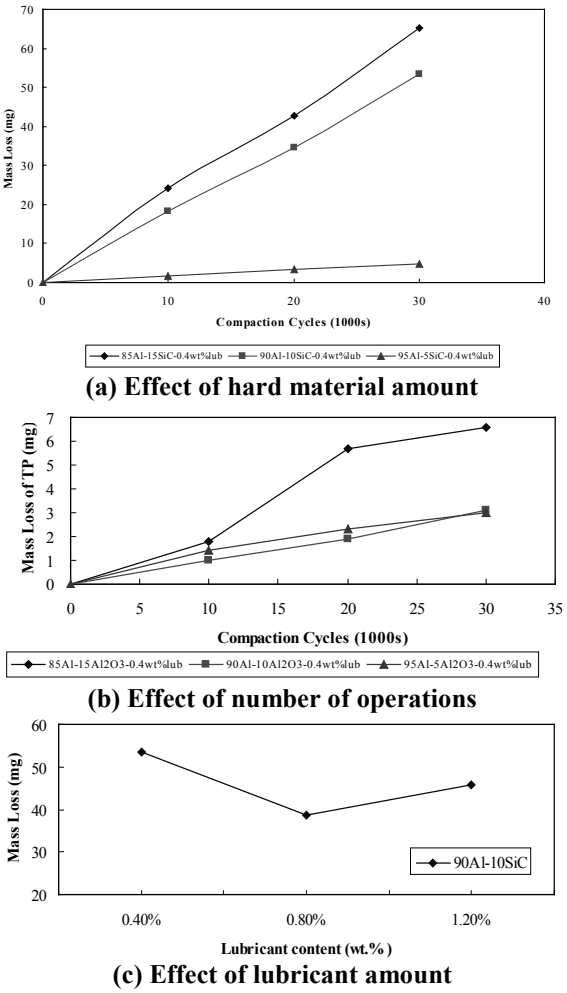

Figure 6. Tool wear measurement through automatic die compaction.

Material Design for Al alloys

We tried to improve mechanical properties of Al alloys. We designed eight Al-based alloys and added Al 6061 powder (Atmix, Japan), recently commercialized using rapid solidification technology. Physical and mechanical properties were measured (density, hardness, tensile strength, elongation and transverse rupture strength) after alloyed samples went through press and sinter processes. We used four control parameters: die compaction pressure, heating rate, sintering temperature, and holding time. Figure 7 shows comparison of transverse rupture strength (TRS) for all Al alloys used in this study.

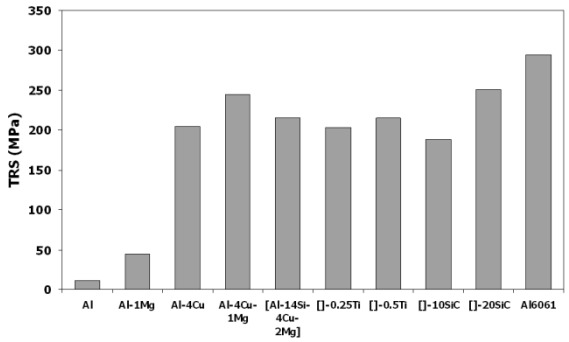

Figure 7. TRS for all Al alloys used in this study.

Bio-Inspired Design for P/M Materials

We developed a new material design by mimicking bamboo, which has a cellular, layered, and fibrous microstructure. These features offer lightweight, high compressive strength and flexibility, which are pre-requisites for superior performance of any automotive component. A finite-element simulation model was developed for three-point-bending test of aluminum alloy with consideration of the effect of porosity on Young's modulus. The results show the bio-inspired design with 30% of porosity has the most beneficial in the strength-to-weight ratio, as shown in Figure 8. We tried several experiments for feasibility study, as shown in Figure 9.

Modeling and Simulation

We used Shima and Oyane model and PMsolver (Cetatech, Inc., Sacheon, Korea) to determine a curve fit for compressibility experimental data of green density versus compaction pressure and simulate die compaction process. The model employs a generalized form of the yield criterion for compaction as follows:

$$\Phi = \left(\frac{q}{\sigma_m}\right)^2 + \alpha(1-D)^{\gamma}\left(\frac{p}{\sigma_m}\right)^2 - D^m$$

where D is the relative density, q is the effective stress, p is the hydrostatic pressure, σ_m is the flow stress of the fully-dense material and α, γ, and m are material parameters. Parameters α, γ, and m are determined by fitting yield-stress data from uniaxial cylindrical compression tests over a range of relative densities. The flow stress, σ_m, of the fully-ense material includes work hardening via a

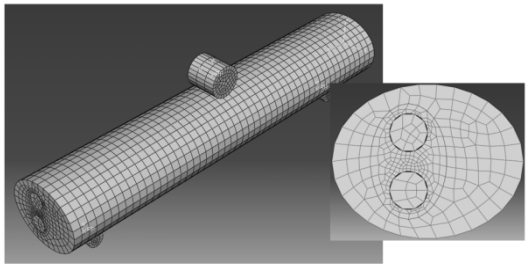

(a) Mesh for three-point bending

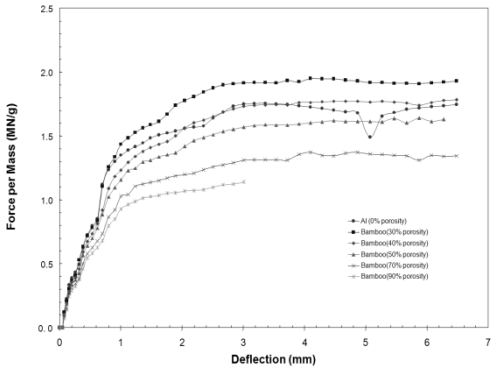

(b) Force per mass plot

Figure 8. Three-point-bending simulation with bamboo-like microstructure.

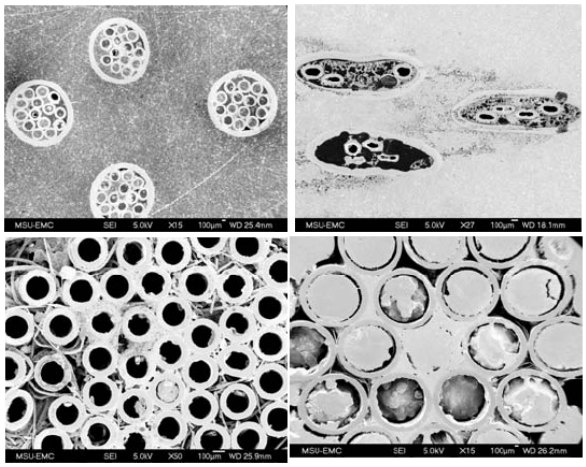

Figure 9. Bamboo-like microstructure of Al and stainless steel.

simple power-law strain relation defined as follows:

$$\sigma_m = a + b\bar{\varepsilon}_m^n$$

where a, b, and n are material parameters and $\bar{\varepsilon}_m$ is the effective strain of the fully-dense material. Figure 10 shows the curve-fitted model for FEM simulation with the amount of lubricant effect.

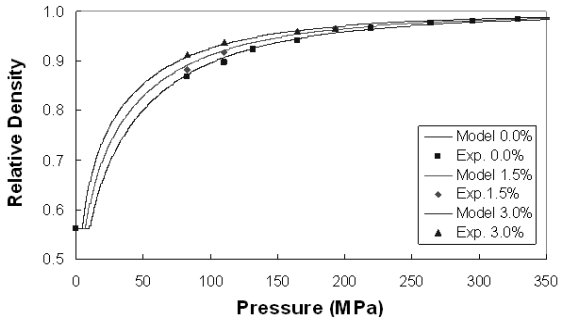

Figure 10. The effect of the amount of lubricant on compressibility of die compaction.

In order to take advantage of our simulation capability, we proposed a new concept of wear work in an integral form based on FEM simulation results of die compaction and ejection.

$$M = H(k_1 S_1 + k_2 S_2)W$$

and

$$W = \int_t \mu \int_A \sigma_n dA v dt$$

where M is the amount of tool wear, H is the Vickers hardess number of tool material, k is the proportional constant, S is the surface area of compact contacted with die tool, subscript 1 is for Al powder and 2 is for hard additives such as alumina (Al_2O_3) or silicon carbide (SiC), W is the wear work, μ is the friction coefficient, σ_n is the normal stress to die tool surface, A is the surface area, v is the velocity of the powder compact and t is the time. We applied this wear work definition to develop FEM simulation tools for die compaction and ejection with experiment validation to investigate the effect of friction coefficient as shown in Figures 11 and 12.

Sensitivity Analysis and Optimization

We performed sensitivity analysis to wear work for five design variables:

- The amount of SiC as hard additives: 2 to 10 kJ/wt%
- The amount of Al_2O_3 as hard additives: 2 to 14 kJ/wt%
- The amount of lubricant: -80 to -150 kJ/wt%
- A fixed friction coefficient: 12 kJ/wt%
- The punch speed of die compaction: 10 to 40 kJ/(m/s)

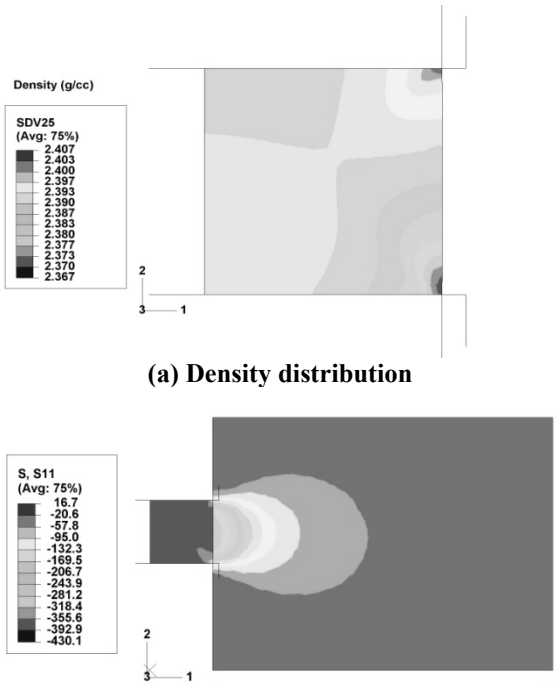

(a) Density distribution

(b) Stress distribution with die tool deformation

Figure 11. FEM simulation result.

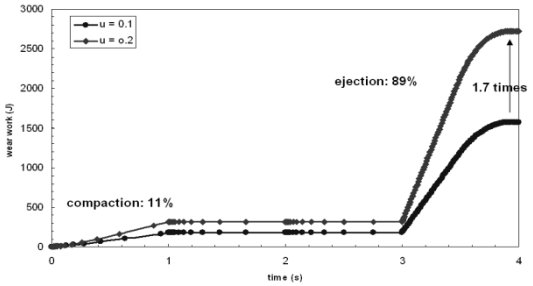

Figure 12. The effect of die compaction and ejection stage with different friction coefficient on tool wear.

To perform the optimization, we need a multi-objective function, including minimization of tool wear, maximization of mechanical property, and minimization of density uniformity; those could be defined based on the user's interest. For each objective function, we needed material parameters to quantify it. Figure 13 shows one example of die-compaction process optimization to maximize density uniformity.

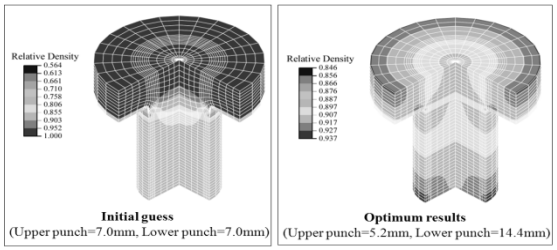

Figure 13. Loading schedule optimization for maximizing density uniformity.

Conclusions

We have accomplished the following tasks:

- Developed a new nondestructive methodology to quantify tool wear for die compaction in the mold using silicon rubber.
- Proposed a new integral equation to quantify tool wear from numerical simulation results.
- Verified the proposed new integral equation to quantify tool wear by automatic compaction experiments and tribological experiments.
- Further studied the impact of lubricant on tool wear.
- Published six journal papers and eleven conference papers related to this task.
- Graduated two students with Master's degrees through this task.

Presentations/Publications/Patents

Journal papers:

1. S. H. Chung, Y.-S. Kwon, S. J. Park, and R. M. German, "Sensitivity Analysis by the Adjoint Variable Method for Optimization of the Die Compaction Process in Particulate Materials Processing," Submitted for publication to ASME J. Eng. Mater. Tech., 2007. (submitted)
2. F. Findik, A. Antonyraj, S. J. Park, and R. M. German, "Investigation of Sintering Behavior and Mechanical Properties of Al P/M Alloys by the Addition of Cu and Mg," *Powder Technology*, 2008. (submitted)
3. F. Findik, A. Antonyraj, S. J. Park, and R. M. German, "Mechanical Properties of Sintered Aluminum Alloys Containing Si, Cu, Mg, Ti, and SiC," *Powder Technology*, 2008. (submitted)
4. J. K. Thompson, W. Li, S. J. Park, A. Antonyraj, F. Findik, and R. M. German, "Utilization of Silicon Rubber to Characterize Tool Surface Quality During Die Compaction," *Powder Metallurgy*, 2008. (accepted)
5. W. Li, P. J. Blau, J. Qu, S. J. Park, and R. M. German, "Tribological Behavior of Die Tool Materials for Powder Metallurgy ," *Powder Metallurgy*, 2008. (under preparation)
6. A. Antonyraj, S. J. Park, and Randall M. German, "Viscoelastic Behavior of Porous Sintered Steels Compact," *Research Letters in Physics*, 2008. (in press)

Conference Presentations:

1. J. K. Thompson, S. J. Park, R. M. German, F. Findik, and A. Antonyraj, **"**Novel Methodology to Quantify Tool Wear in Powder Metallurgy," *Proceedings of the 2007 International Conference on Powder Metallurgy & Particlate Materials (PowderMet 2007)*, complied by John Engquist and Thomas F. Murphy, Metal Powder Industries Federation and APMI International, Princeton, NJ, USA, Part 1, pp. 50–59, Denver, CO, USA, May 13–16, 2007.
2. A. Antonyraj, S. J. Park, and R. M. German, "Thermal Expansion and Viscoelastic Properties of Sintered Porous Ferrous Components," *Proceedings of the 2007 International Conference on Powder Metallurgy & Particlate Materials (PowderMet 2007)*, complied by John Engquist and Thomas F. Murphy, Metal Powder Industries Federation and APMI International, Princeton, NJ, USA, Part 1, pp. 60–69, Denver, CO, USA, May 13–16, 2007.
3. F. Findik, J. K. Thompson, A. Antonyraj, S. J. Park, and R. M. German, **"**Mechanical and Physical Properties of Titanium and Silicon Carbide Containing Mixed Powder Sintered Aluminum," *Proceedings of the 2007 International Conference on Powder Metallurgy & Particlate Materials (PowderMet 2007)*, complied by John

Engquist and Thomas F. Murphy, Metal Powder Industries Federation and APMI International, Princeton, NJ, USA, Part 10, pp. 103–113, Denver, CO, USA, May 13–16, 2007.

4. F. Findik, A. Antonyraj, S. J. Park, and R. M. German, "Investigation of Sintering Behavior and Mechanical Properties of Al P/M Alloys by the Addition of Cu and Mg," *5th International PM Conference*, Ankara, Turkey, October 8–12,.2008.
5. A. Antonyraj, P. Suri, S. J. Park, G. Thibaudeau, R. M. German, B. Brain, and K. Cho "Development Novel Bio-Inspired Design Ferrous Components," *Bio Inspired Design 2008 Conference*, August 19–22, Mississippi State, MS.
6. A. Antonyraj, S. J. Park, G. Thibaudeau, R. M. German, and B. Brain "Fabrication of Bio-Inspired Design Engineering Components by Powder Metallurgy," *Bio Inspired Design 2008 Conference*, August 19–22, Mississippi State, MS.
7. A. Antonyraj, P. Suri, S. J. Park, and R. M. German, "Development and Analysis of Bio-inspired Design Aluminum Composites," *PM 2008*, Washington, D.C., USA, June 8–12, 2008.
8. W. Li, P. J. Blau, J. Qu, S. J. Park, Y. Hammi, and R. M. German, "Prediction of Tool Wear and Tool Life by Experiment/ Modeling/ Simulation of the Die Compaction Process," *PM 2008*, Washington, D.C., USA, June 8–12, 2008.
9. S. Lee, H. Singh, S. J. Park, S. Atre, and R. M. German, "Mapping between Material Design and Properties Using Material Informatics for P/M Simulation," PM 2008, Washington, D.C., USA, June 8–12, 2008.
10. Antonyraj, S. J. Park, R. M. German, P. Suri, W. Morgan, T. Pelletiers, Y. Kato, and I. Otsuka, "Mechanical Properties of Various Aluminum Alloys by Powder Metallurgy," TMS 2008, New Orleans, LA, USA, March 9–13, 2008.
11. A. Antonyraj, S. J. Park, R. M. German, P. Wang, T. Pelletiers, Y. Kato, and I. Otsuka, "Mechanical Properties of Aluminum 6061 Alloys by Powder Metallurgy," TMS 2009, San Francisco, CA, USA, February 15–19, 2009.